ENVIRONMENTAL IMPACTS OF URBANIZATION ON MAJOR CITIES OF PUNJAB, PAKISTAN

Project/Thesis ID. 2023: 111

Session: BSc. Fall 2019-2023

Project Supervisor: Mr. Arsalan Raza

Submitted By:

Imran Sikander

Tanveer Waheed

Munim Ahmed

Muhammad Zargham

Department of Civil Engineering

Wah Engineering College

University of Wah

Certification

This is to certify that **Imran Sikander**, **UW-19-CE-BSC-033**, **Tanveer Waheed**, **UW-19-CE-BSC-010, Munim Ahmed**, **UW-19-CE-BSC-041** and **Muhammad Zargham**, **UW-19-CE-BSC-012** have successfully completed the final project **Environmental impacts of urbanization on major cities of Punjab, Pakistan,** at the **Civil Engineering Department, Wah Engineering College, University of Wah**, to fulfill the partial requirement of the degree **BSC Civil Engineering.**

External Examiner	**Project Supervisor**
[Name of Examiner]	[Mr. Arsalan Raza]
[Designation]	[Lecturer]

Chairman

Department of Civil Engineering, University of Wah

Environmental impacts of urbanization on major cities of Punjab, Pakistan

Sustainable Development Goals

SDG No	Description of SDG	SDG No	Description of SDG
SDG 1	No Poverty	SDG 9	Industry, Innovation, and Infrastructure
SDG 2	Zero Hunger	SDG 10	Reduced Inequalities
SDG 3	Good Health and Well Being	✓ SDG 11	Sustainable Cities and Communities
SDG 4	Quality Education	SDG 12	Responsible Consumption and Production
SDG 5	Gender Equality	✓ SDG 13	Climate Change
SDG 6	Clean Water and Sanitation	SDG 14	Life Below Water
SDG 7	Affordable and Clean Energy	SDG 15	Life on Land
SDG 8	Decent Work and Economic Growth	SDG 16	Peace, Justice and Strong Institutions
		SDG 17	Partnerships for the Goals

Range of Complex Problem Solving			
	Attribute	**Complex Problem**	
1	Range of conflicting requirements	Involve wide-ranging or conflicting technical, engineering and other issues.	
2	Depth of analysis required	Have no obvious solution and require abstract thinking, originality in analysis to formulate suitable models.	✓
3	Depth of knowledge required	Requires research-based knowledge much of which is at, or informed by, the forefront of the professional discipline and which allows a fundamentals-based, first principles analytical approach.	✓
4	Familiarity of issues	Involve infrequently encountered issues	
5	Extent of applicable codes	Are outside problems encompassed by standards and codes of practice for professional engineering.	
6	Extent of stakeholder involvement and level of conflicting requirements	Involve diverse groups of stakeholders with widely varying needs.	
7	Consequences	Have significant consequences in a range of contexts.	✓
8	Interdependence	Are high level problems including many component parts or sub-problems	✓
Range of Complex Problem Activities			
	Attribute	**Complex Activities**	
1	Range of resources	Involve the use of diverse resources (and for this purpose, resources include people, money, equipment, materials, information and technologies).	✓
2	Level of interaction	Require resolution of significant problems arising from interactions between wide ranging and conflicting technical, engineering or other issues.	✓
3	Innovation	Involve creative use of engineering principles and research-based knowledge in novel ways.	✓
4	Consequences to society and the environment	Have significant consequences in a range of contexts, characterized by difficulty of prediction and mitigation.	✓
5	Familiarity	Can extend beyond previous experiences by applying principles-based approaches.	✓

Abstract

Urbanization is a rapidly growing global trend, with a significant impact on the environment and human health. Understanding the patterns of urbanization and their associated impacts is critical to mitigating these effects. Urban Heat Island (UHI) is a widely studied phenomenon in which urban areas exhibit higher temperatures than their rural surroundings. The UHI phenomenon has been linked to a range of negative impacts, including increased energy consumption, air pollution, and adverse health effects. In this study, we examined the urbanization patterns in the Districts of Lahore, Rawalpindi, Faisalabad, and Multan from 2000 to 2020 using USGS Landsat data. We utilized USGSLandsat 4, 6, and 7 data to analyze changes in land use and land cover (LULC) in these Districts. Our results highlight the beneficial impact of green spaces in urban environments. We categorized the study areas into four classes, namely built-up, barren land, vegetation, and water bodies. Over the past two decades, an increase in surface temperature of 2°C was observed in Rawalpindi, and 2.4°C and 2.6°C in Multan and Lahore respectively. Also, a significant decrease was seen percentage of waterbodies, and an increase was observed in percentage of built-up areas in the study districts. Additionally, we applied an Artificial Neural Network (ANN) through Python to estimate future surface temperature changes from 2020 to 2050, and found an expected increase of 4°C, 2°C, 1.5°C, and 3.5°C in Lahore, Multan, Rawalpindi, and Faisalabad Districts, respectively. Our study highlights the importance of effective urban planning to control urbanization and mitigate the impacts of UHI. By analyzing the LULC changes and estimated future surface temperature increases, our study provides valuable insights for policymakers and urban planners to develop sustainable urbanization strategies that prioritize the creation of green spaces and the protection of natural areas to mitigate the UHI effect.

Keywords: Urbanization; USGS; UHI; LULC

Undertaking

I certify that the project **Environmental Impacts of Urbanization of population on major cities of Punjab, Pakistan** is our own work. The work has not, in whole or in part, been presented elsewhere for assessment. Where material has been used from other sources it has been properly acknowledged/ referred.

[Imran Sikander]
[**Uw-19-ce-bsc-033**]

[Tanveer Waheed]
[**Uw-19-ce-bsc-010**]

[Munim Ahmed]
[**Uw-19-ce-bsc-041**]

[Muhammad Zargham]
[**Uw-19-ce-bsc-012**]

Acknowledgement

We truly acknowledge the cooperation and help made by **Mr. Arsalan Raza, lecturer** of **Wah Engineering College, University of Wah.** He has been a constant source of guidance throughout the course of this project. We would also like to thank **Mr. Taimur Sheikh** from **Wah Engineering College, University of Wah** for his help and guidance throughout this project.

We are also thankful to our friends and families whose silent support led us to complete our project.

TABLE OF CONTENTS

Contents

List of Tables

List of Figures

List of Acronyms

LU: Land Use

LC: Land Cover

NDVI: Normalized Difference Vegetation Index

API: Air Pollution Index

LST: Land Surface Temperature

UHI: Urban Heat Island

PD: Population Density

NDBI: Normalized Difference Built-Up Index

NDWI: Normalized Difference Water Index

ANN: Artificial Neural Network

Chapter 1

1.1 Background

Pakistan ranks below Indonesia as the fifth-largest nation by population, with a growth rate of 1.91% and a population density of 267/km². Urban regions' economic growth and social functions have significantly changed as a result of the rapid industrialization and urbanization processes[1].Modern cities have experienced hasty and haphazard urbanization, particularly over the past three decades as the population has increased everywhere, including in Pakistan[2]. This has led to environmental issues such as rising energy consumption, changes in the climate of the region, an increase in LST and LC, and higher levels of AQI values.

Urban environments are prone to a phenomenon called "heat island." The urban atmosphere's constant temperature increase, a rise in air pollutants like NO_x and SO_x, and a reduction in relative humidity are just a few of its characteristics. Urban heat islands, which cause surface temperatures and overall ambient temperatures to rise, are a phenomenon that happens when cities replace the natural land cover with dense concentrations of pavement, buildings, and other surfaces that absorb and retain heat[3]. It has been studied using both observational and numerical methods.

The most extensively researched and studied factor affecting the climate is probably environmental change. The nature of climate change makes it unavoidable and unstoppable. However, anthropological impacts including the combustion of fossil fuels, excessive greenhouse gas emissions, and urbanization have been directly connected to 20th-century global warming[4].

Here are some reasons why studying urbanization is important:

1. **<u>Population Growth:</u>** Population growth is significantly influenced by urbanization since more people are moving to cities. By researching urbanization, we may better understand how cities are developing and how they might be designed and managed to serve a growing population may by studying urbanization[5].

2. **<u>Social and Economic Development:</u>** Urbanization may result in more rapid social and economic development. Greater demand for goods and services as a result of more people relocating to cities can generate employment opportunities and boost economic growth. We can better grasp how cities contribute to economic growth and social transformation by

studying urbanization[6].

3. **Environmental Impacts**: Significant environmental effects of urbanization include the loss of natural ecosystems, water pollution, and air pollution[7]. We are able to better understand these effects and create plans to reduce them by studying urbanization.

4. **Urban Planning:** Cities and towns' physical development, including land use, transportation, and infrastructure, is impacted by urbanization. We can develop more effective, livable, and sustainable city plans and designs by examining urbanization[8].

5. **Public Health:** Public health is significantly impacted by urbanization, including factors like access to healthcare, pollution exposure, and the spread of infectious diseases. We can better understand the health dangers of residing in cities and create mitigation methods by studying urbanization[9].

1.2 Problem Statement

The average temperature of an urban area rises due to anthropogenic activities, as a consequence, it creates an Urban Heat Island effect, that imparts unfavorable outcomes on the environment and living beings in terms of increase in air pollution levels as well as increase in land surface temperature.

1.3 Objectives

The project's overall goal is to determine the effect of urbanization on major cities in Pakistan. The following are the precise goals:

- To develop the relationships of land surface temperature with Vegetation Area, Built up Area, Water Area, and Rainfall.
- To predict the Land Use Land Cover and Land Surface Temperature using Machine Learning Techniques
- To evaluate the mitigation strategies to reduce urban heat island phenomena in urban areas.

1.4 Limitations of the study

To avoid complexity, the limitations of this study are:

- The data from different regions of the country was not accessible for us to work upon.
- The data we used for the study might not be precise to certain range.

1.5 Methodology

- Literature Review.
- Collection of data through USGS Earth Explorer, Data Access NASA and Google Engine for different parameters such as NDBI, NDVI, NDWI, PD, Rainfall, LULC, LST of year 2000 to 2020 for our study areas.
- Studied the co-relation b/w different parameters with LST.
- Through ANN model, we have predicted the LST, UHI and LULC mapping for year 2040 and 2050.
- Interpretation of Results.
- Recommendations.

1.6 Project Layout

The report is composed of five chapters. These are as follows:

Chapter 1: The introduction to the topic is given. It assesses the project's motivation, and problem description. It focuses on the overall aims, usual goal, and research limits in particular. It contains a basic approach as well as document format information.

Chapter 2: A thorough literature review is provided. In this section, we will examine prior procedures for studying environmental impacts like LC. Rainfall, Wind data, LST, and NDVI data are used by various researchers, keeping urbanization in view.

Chapter 3: It describes the research approach and methodology to be followed in order to complete the desired project.

Chapter 4: After performing various tests the results and discussions are presented.

Chapter 5: Conclusions and recommendations are provided on the basis of results.

Chapter 2

2.1 Introduction

The goal of reviewing previously published research papers was to find out what research has been done on the topic of "Environmental Impacts of Urbanization on major cities of Pakistan," which is directly related to the environment and temperature variation of certain area. In this chapter, we'll look at the Causes and effects of UHI, different factors which have impart effect on the environment and shows variation in temperature. Sustainability and urban management are closely linked as urban areas are responsible for a significant portion of global energy consumption, greenhouse gas emissions, waste production, and natural resource consumption. Therefore, urban management practices play a crucial role in ensuring the sustainability of cities and their surrounding regions.

Urban management encompasses a range of activities, including urban planning, land use management, transportation planning, energy management, waste management, and water management. By implementing sustainable urban management practices in each of these areas, cities can reduce their environmental impact, improve quality of life for residents, and enhance economic development. Sustainable land use management practices can help preserve natural areas and protect biodiversity. This can include the establishment of parks, green roofs, and urban gardens, as well as the use of sustainable building materials and practices.

2.2 UHI

Urban heat island is a phenomenon that occurs when cities replace the natural land cover with dense concentrations of pavement, buildings, and other surfaces that absorb and retain heat[10][11].

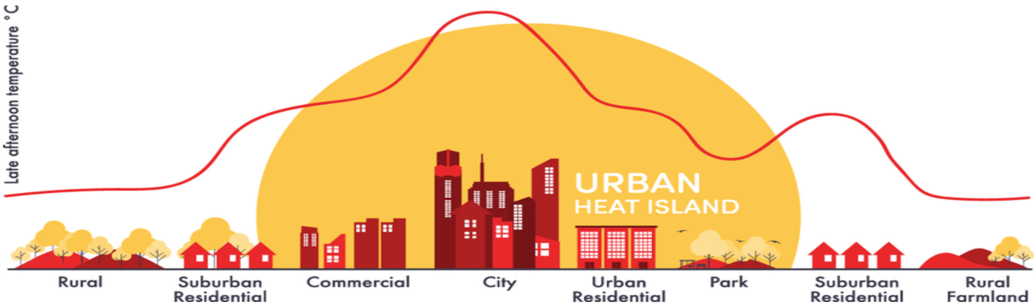

Figure2.1 Temperature of different areas. (Source: https://community.wmo.int/activity-areas/urban/urban-heat-island)

Figure 2.1 shows that the city's temperature is higher than that of the same area, mostly as a result of the city's high population density and the quantity of construction materials needed to create infrastructure, such as pavements.

2.3 Causes of UHI

For the purpose of creating efficient mitigation plans and advancing sustainable urban planning and design, it is essential that we understand the causes of UHI. The UHI is impacted by a number of factors; some of them are as follow:

2.3.1 Use of construction materials

Concrete and asphalt are two building materials that have large heat capacities and absorb a lot of solar radiation. They can absorb and store a lot of heat during the day when these materials are widely employed in urban areas for buildings, sidewalks, and roadways. In turn, this causes urban surfaces to heat up, raising local temperatures and causing the UHI effect[12].

2.3.2 Reduction of green cover

Through a process known as evapotranspiration, vegetation, in particular, plays a critical role in controlling temperatures. By collecting and releasing heat, this mechanism aids in cooling the surrounding air. Evapotranspiration reduces as the amount of green cover is decreased, which leads to less cooling of the urban environment and higher temperatures nearby, intensifying UHI [13].

2.3.3 Anthropogenic heat emission

The Urban Heat Island (UHI) effect is significantly influenced by anthropogenic activities, which are defined as human-initiated activities and processes. These activities affect land surfaces and increase energy use and pollutant discharge, which all have an impact on UHI[11].

2.4 Effects of UHI

Urban areas and the people who live there are significantly impacted by the Urban Heat Island (UHI) phenomena. Understanding the effects of UHI is essential for putting mitigation measures in place to create stronger and more sustainable cities. Some of the effects of UHI are as follow:

2.4.1 Building energy consumption

In comparison to nearby rural areas, UHI raises the temperature in metropolitan areas. Buildings in urban areas consequently endure higher outside temperatures. The need for cooling within buildings to maintain suitable interior temperatures rises as a result of this heat accumulation[14]. To combat the higher ambient temperatures brought on by UHI, buildings need to consume more energy for air conditioning systems, fans, and other cooling methods.

2.4.2 Air Pollution

UHI can have an impact on how people think and behave, which can enhance some pollution sources. For instance, increased use of automobiles or power generation may occur during heat waves or other times of extreme heat, leading to a rise in emissions and air pollution[15]. The release of volatile organic compounds (VOCs) from sources like industrial operations, car emissions, and chemical solvents can also be impacted by the UHI effect. To create secondary pollutants like ozone and particle matter, VOCs can react with other contaminants.

2.4.3 Global Warming

Due to increasing energy use, transportation emissions, and industrial activity, urban areas with UHI typically have greater concentrations of greenhouse gases such carbon dioxide (CO_2) and methane (CH_4). The greenhouse effect, which results from these greenhouse gases trapping heat in the atmosphere, accelerates global warming. Therefore, the heat buildup from UHI has the potential to amplify the greenhouse effect and contribute to the planet's overall warming[16].

2.4.4 Heat-related diseases

Urban regions experience greater ambient temperatures than the nearby rural areas due to UHI. Heat-related illnesses can result from the body's inability to control its temperature due to the excessive heat. Heat exhaustion, heatstroke, and other heat-related conditions can be brought on by prolonged exposure to high temperatures, especially during heat waves[17].

2.5 Population Census for Major Cities of Pakistan

The following table shows the population of major cities in Pakistan of 1998 and 2017 respectively:

Table2.1 Population data of different cities in Pakistan.

Sr.no	City	Population in 2017 (Millions)	Population in 1998 (Millions)	% Change
1	Lahore	11.12	5.14	113.59
2	Faisalabad	3.20	2.01	59.05
3	Multan	1.87	1.19	56.08
4	Rawalpindi	2.09	1.41	48.5

As you can see in Table 2.1 that disastrous change in population has occurred from year 1998 to 2017 which will change environmental factors (LC, LST, LU) in a way as well.

Table 2.2 Population data for different provinces of Pakistan.

Sr.no	Province	Population in 2017 (Millions)	Population in 1998 (Millions)	% Change
1	KPK	30.50	17.74	71.94
2	Punjab	109.98	73.62	49.39
3	Sindh	47.85	30.43	57.21
4	Balochistan	12.33	6.56	87.86

2.6 Relevant Work

Sohail et al studies that due to a variety of circumstances, including industrial expansion, economic growth, and other related developments, rural-urban migration is a significant phenomenon today. Because it reduces the amount of greenery inside and surrounding the cities, this rapid urban expansion is extremely complex in nature[18]. The environment and ecosystem of the first decade of the twenty-first century suffered greatly from the rapid urbanization. Given that there is an annual increase in the global urban population, the population growth rate is particularly crucial[19].Urbanization causes the biophysical environment to change, impermeable urban materials to replace natural land coverings, negative effects on land surface features, and changes to land surface energy processes[20].

Ullah K. et al [21] studied that the natural environment has been significantly impacted by patterns of global economic development over the past three decades, and economies have experienced a wide range of environmental challenges as a result of the harmful effects of climate change. Pakistan is the sixth most vulnerable nation among them, and the country's socioeconomic and ecological conditions have been negatively impacted by climate change. In this regard, this study used an annual time series dataset ranging from 1990 to 2020 to examine the role of green energy consumption, eco-innovation, and urbanization while outlining the dream of a low-carbon economy and environmental sustainability in the context of Pakistan[22].

Sajid M. et al [23] studied the phenomena of urbanization in Pakistan, a developing nation, is dealing with a rapidly growing urbanization that greatly benefits its citizens. When it gets unmanageable, it simultaneously strives to affect the environment negatively. One of the main issues with urbanization is that it raises the ambient temperature, which unluckily causes UHI and ultimately worsens the environment in metropolitan areas[24].

Sanjeev et al studied that achieving the Sustainable Development Goals (SDGs) depends on accurate determine of the microenvironment, radiate susceptibility, and forecasting of climate and weather scenarios in urban settings. Urban Heat Islands (UHIs) are a result of rapid urbanization's major effects on both the local and global atmosphere[25].

Kaveh et al studied the causes and effects of UHI Despite the fact that research on the urban heat island (UHI) impact has grown tremendously over the past few decades; the literature hardly ever reports a systematic analysis of the components that contribute to the UHI effect. The various spatial and temporal elements influencing the UHI impact are systematically and comprehensively reviewed in this work [26]. UHI is a phenomenon that occurs when urban areas have hotter temperatures than the non-urban areas around them. It is thought to be a major contributor to global warming, heat-related deaths, and unpredictable climatic fluctuations [27]. Therefore, it is crucial to pinpoint the spatio-temporal elements that influence (or alleviate) the UHI effect in order to fully comprehend their causal mechanisms and devise urban planning strategies to address them [28].

Kafy et al studied that the maximum prospect method is used to determine the land-use and land-cover pattern supervised classification. For the research region, a total of four classes—built-up, barren Land, vegetation, and water bodies—were mapped [29]. Spectral radiance has been converted to effective sensor brightness temperature using Plank's reverse function. The land surface temperature (LST) is determined using Normalize Difference Vegetation Index (NDVI) classes based on surface emissivity. The city's built-up regions and arid plains saw the highest temperatures, while places with more greenery experienced the lowest temperatures [30]. The land surface temperature views make the existence of UHI temperature abundantly clear. District Lahore has seen an increase in surface temperature of 2°C during the past 20 years. In the past 19 years, the surface temperatures in the districts of Faisalabad and Multan have risen by 2.2°C and 2.4°C, respectively [31].

Mohsin et al studied that, regarding assessing and controlling the rising temperatures in metropolitan areas, regulating agencies and governments at global and regional sizes have made the effects of climate change felt around the world a priority .In order to forecast future impact patterns of LST and LULC, this study examined the temporal variability in urban microclimate in terms of land surface temperature (LST) and its link with changes in land use and land cover (LULC) in Lahore city. The Landsat Thermal Infrared Sensor (TIRS) and the land surface emissivity factor were used to calculate the LST variability[32]. Landsat satellite data from 1992 to 2020 was used to examine the impact of LULC utilizing the normalized difference vegetation index (NDVI) and the normalized difference building index (NDBI) on the variability LST. Urban LST and LULC class influence were calculated using pixel-level multivariate linear regression technique. The findings showed that from 1992 to 2020, there was an overall rise in built-up areas of 41.8% at a rate of declines in vegetation, bare ground, and water of 24%, 17.4%, and 0.4%, respectively. A large amount of consistency may be seen when comparing LST acquired from the meteorological station with satellite photos .The temperature in built-up regions increased by 4.3°C between 1992 and 2020. The same were projected for 2025 and 2030 based on LULC and LST trends, which showed that LST may further increase up to 1.3 C by 2030[33].

Sajjad et al analyzed that, the expansion of buildings has a noteworthy influence on land use/land cover (LULC) due to conversion of vegetation land into commercial and residential areas and their associated infrastructure by which LST is accelerated[34]. The objective of the research was to study the impact of changes in LULC on LST of Southern Punjab (Pakistan) through remote sensing (RS) data. Landsat images of 30-year duration (1987, 1997, 2007 and 2017) were employed for identifying vegetation indices and LST in the study region. These images also helped to work out normalized difference water index (NDWI) and normalized difference built-up index (NDBI) maps. There was an increase from 29620 (3.63 %) to 88038 ha (10.8 %) in built-up area over the 30 years. LST values were found in the range 12–42 °C, 11–44 °C, 11–45 °C and 11–47 °C in the years 1987, 1997, 2007 and 2017, respectively. Regression coefficients (R_2) 0.81, 0.78, 0.84 and 0.76 were observed between NDVI and LST in the corresponding years respectively. Our study showed that NDVI and NDWI were negatively correlated with less LST; however, NDBI showed positive correlation with high LST[35].

Tariq et al studied that, intends to evaluate the urbanization of Lahore, Pakistan's second-largest city, and its effects on land surface temperature(LST)[36]. Different normalized satellite indices and geographic information system (GIS) and remote sensing (RS) approaches have been used in this study to analyze the spatiotemporal patterns of Lahore city utilizing Landsat data from 1990, 2004, and 2018. New tools for analyzing changes in land use and land cover have been made possible by the development of integrated usage of RS and GIS, combined cellular automata-Markov models, and trajectory projection. According to the findings, the built-up area and bare land grew from 15,541 (27%) to 23,024 km^2 (40%) and from 5756 km^2 (10%) to 13,814 km^2 (24%), respectively. In the meantime, the area covered by water and vegetation declined from 33,961 km^2 (59%) to 19,571 km^2 (34%) and from 2302 km^2 (4%) to 1151 km^2 (2%) correspondingly. This urbanization also had an impact on the city's LST. Most of the region's mean LST was between 14 and 28 °C in 1990, but it increased to between 22 and 28 °C in 2004 and between 34 and 36 °C in 2018. Each land use land cover (LULC) class has a different surface reflectance and roughness due to the shifting vegetation and built-up land. The investigation found that the Normalized difference Water Index (NDWI), Normalized Difference Vegetation Index (NDVI), and LST are directly correlated[37].

Liu et al studied that urban green and blue infrastructures (GBI) are seen to be a useful tool for reducing heat stress and enhancing thermal comfort in cities. The thermal effects of the primary GBI forms, such as trees, green roofs, vertical greenings, and water bodies, have been the subject of several researches. The resulting heat effects may vary depending on the individuals' physical attributes, planting strategies, and local urban fabric characteristics. A key tool in GBI research is ENVI-met, a comprehensive three-dimensional modeling program that can accurately mimic the outdoor microclimate. The GBI studies use this technology to conduct their three-step research process, which entails modeling, validation, and scenario simulation. A thorough review of GBI-targeted studies was carried out using ENVI-met as the main instrument in order to provide a systematic and overall evaluation of the current research workflow. In their modeling, validation, and scenario simulation processes, the results of 79 peer-reviewed papers were examined and synthesized. An emphasis was placed on closely investigating their data sources, assessing indicator choices, analyzing key analytical stances, and distilling suggestions to enhance the research workflow. This study offers suggestions for improving research on GBI thermal impacts as well as an explanation of the ENVI-met technique[38].

Hadi et al studied the concepts of using machine learning techniques to enhance the prediction process results using ANN model. In this study, an artificial-neural-network-based cellular automaton (ANN-CA) model is used to simulate and forecast changes in LULC in North Sumatra, Indonesia. High agreement can be seen when comparing the real and predicted LULC maps for 2010, with a Kappa index of 0.83 and an accuracy rating of 87.28%. The ANN-CA model is then used to forecast changes in LULC in 2050 and 2070. The LULC estimates show significant increases in plantation area of more than 4% for the years 2050 and 2070. By 2050, it is anticipated that the area dedicated to crops and forests will have decreased by 1.2% and 1.6%, respectively. Forest and cropland will decrease by 1.2% and 1.7%, respectively, by 2070, showing that plantations will be the main human influence on LULC as opposed to forests and crops[39].

Ullah et al studied that, the land surface temperature (LST) in the area increased as a result of the LULC shift[40]. Using Landsat data and the support vector machine (SVM) approach, LULC and LST changes were evaluated for the time span 1990–2017. Using a transition potential matrix derived from the data years of 2002 and 2017, a combined cellular automata and artificial neural network (CA-ANN) prediction model was utilized to simulate LULC changes for the time periods of 2032 and 2047. Using validation modules in QGIS, the CA-ANN model's accuracy was tested using simulated and categorized photos from 2017, with a 70% correctness rate. LST was derived using the temperature bands of Landsat photos taken in 1990, 2002, and 2017. The LST gathered for this time period was then modeled for 2032 and 2047 using linear regression analysis and urban indices (UI). According to the SVM land cover classification results, between 1990 and 2017, built-up area increased by 5.75%, bare soil increased by 4.22%, and vegetation decreased by 9.88%. The built-up area has the greatest mean LST compared to other classes, according to the LST results for LULC classes. According to LULC and LST's projections for the future, of the overall LULC area, which was less than 11% in 2017, the built-up area may rise by 12.48% and 14.65% in 2032 and 2047, respectively[41].

Chapter 3

3.1 Introduction

Urbanization is increasing in Pakistan, a developing nation, and it is having a good effect on the population. When it can no longer be controlled, it also damages the ecosystem. One of the primary issues with urbanization is that it raises the ambient temperature, which unluckily causes UHI and ultimately damages the environment in urban areas. This study provides thorough knowledge regarding the relationship among land surface temperature and vegetation, built-up areas, water areas, and rainfall, which aids in the evaluation of mitigation measures to minimize the urban heat island phenomenon in urban areas.

3.2 SCHEMATIC PLAN OF PROJECT

The schematic plan of our project is as follow:

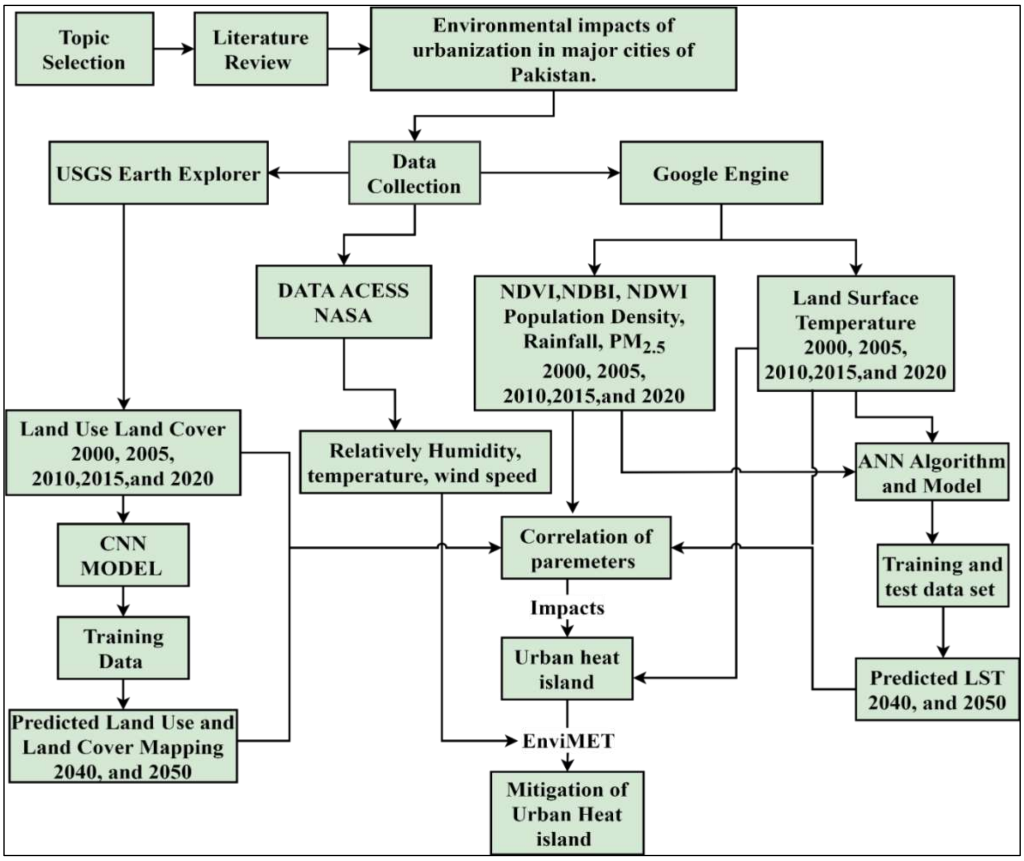

Figure3.1 Methodology Flow Chart.

3.3 Study Area

Districts of Multan, Lahore, Rawalpindi, and Faisalabad have been selected as study areas for our project as they are the districts of Punjab province whose population is around 110 million in 2017 which is comparatively quite high from other provinces as shown in table 2.2. These districts are solely selected on the basis of population growth from the year 1998 to 2017 in Punjab province as shown in table 2.1 [31].

Table 3.1 Percent change in Population growth from 1998 to 2017.

Sr.no	City	Population in 2017 (Millions)	Population in 1998 (Millions)	% Change in population	Latitudes	Longitudes
1	Lahore	11.12	5.14	113.59	31.588° N	74.356° E
2	Faisalabad	3.20	2.01	59.05	31.451° N	73.089° E
3	Rawalpindi	2.09	1.41	48.5	33.606° N	73.056° E
4	Multan	1.8	1.19	56	30.196° N	71.478° E

3.4 Methodology

3.4.1 Materials and Methods

For the purpose of conducting this study, a set of selected urban parameters, including the collection of satellite data, image classification, creation of land use and land cover maps, creation of NDVI maps, retrieval of LST, relationship assessment between LST and built-up areas, and relationship assessment between LST and green spaces, were used. However, the Google Earth Engine platform was employed for LST purposes because it is the interface through which we may use and get data and achieve the desired results using the LST technique.

3.4.2 Coding on Google Earth Engine

We have done coding on the Google earth engine for the extraction of data of LULC, Rainfall, PD, LST, NDBI, NDVI, NDWI, and $PM_{2.5}$ using Landsat data from Landsat 5, Landsat 7 and Landsat 8 for the years 2000 to 2020.

3.4.2.1 NDBI

Normalized Difference Built-up Index (NDBI) is a commonly used remote sensing index to map and monitor urbanization and land use changes in urban areas. A measure of the proportion of built-up and unbuilt-up regions in an urban area, NDBI is generated from satellite photography. The index distinguishes between built-up and unbuilt-up environments using the near-infrared (NIR) and shortwave-infrared (SWIR) bands. While the SWIR band is sensitive to built-up surfaces, the NIR band is sensitive to vegetation and undeveloped areas. The NDBI can successfully differentiate between built-up and unbuilt-up areas by calculating the difference between these two bands[42]. Studies examining the effects of urbanization on land use, environmental quality, and public health have frequently used NDBI[43]. In Pakistan, NDBI has been utilized to examine urban growth and changes in land use in significant cities including Lahore, Karachi, and Islamabad. The formula for NDBI is,

NDBI = (SWIR - NIR) / (SWIR + NIR) **(Equation 3. 1)**

```
// Sentinel-2/Landsat 5 Normalized Difference Vegetation Index (NDBI) script,

var ndbi_palette = 'FFFFFF, CE7E45, DF923D, F1B555, FCD163, 99B718, 74A901, 6

//Landsat 5 (1984-2012)

var L5_display = {bands: ["B3", "B2", "B1"], min: 0, max: 0.5};

function addndl5(input) {
  var nd = input.normalizedDifference(['B5', 'B4']).rename('ndbi');
  return input.addBands(nd);
}

var L5_collection = ee.ImageCollection("LANDSAT/LT05/C01/T1_TOA")
  .filterBounds(geometry)
  .filterDate('1990-01-01', '1990-12-31')
  .filter(ee.Filter.lt("CLOUD_COVER", 0.1))
  .map(addndl5);

print(L5_collection);

var L5_mosaic = L5_collection.median().clip(geometry);

Map.addLayer(L5_mosaic, L5_display, "Landsat 5",false);

var ndbi_L5 = L5_collection.select('ndbi').median().clip(geometry);

Map.addLayer(ndbi_L5, {min: -0.1, max: 1, palette: ndbi_palette}, 'NDbI L5');
Map.centerObject(geometry);

Export.image.toDrive({
  image: ndbi_L5,
  description: 'NDBI_Landsat-2005',
  fileNamePrefix: 'NDBI_L5_',
  folder: 'Bhawalpurr',
  scale: 30,
  maxPixels: 1e13,
  region: geometry
});
```

Figure 3.2 Code of NDBI

3.4.2.2 NDVI

The term "normalized difference vegetation index," or "NDVI," refers to a remote sensing metric used to assess the health and greenness of vegetation. The near-infrared (NIR) and red light bands of satellite imagery are compared for reflectance to get the NDVI[44]. In contrast to ill or sparse vegetation, which reflects less NIR and absorbs fewer red lights, healthy vegetation reflects more NIR. NDVI values can be produced that range from -1 to +1 by taking the difference between the NIR and red bands and dividing it by their combined value. Lower NDVI values signify sparse or non-vegetated environments, while higher values signify healthier and denser vegetation. In studies conducted in Pakistan, NDVI has been used to monitor changes in plant cover brought on by urbanization and changes in land use, as well as to assess how climate change is affecting agricultural productivity and vegetation growth. The formula for NDVI is,

NDVI = (NIR - Red) / (NIR + Red) **(Equation 3. 2)**

```
▸ var geometry: Table users/uw-19-ce-bsc-033/Bhawalpurr
// Sentinel-2/Landsat 5 Normalized Difference Vegetation Index (NDVI) script

var ndvi_palette = 'FFFFFF, CE7E45, DF923D, F1B555, FCD163, 99B718, 74A901,

//Landsat 5 (1984-2012)

var L5_display = {bands: ["B3", "B2", "B1"], min: 0, max: 0.5};

function addndl5(input) {
  var nd = input.normalizedDifference(['B4', 'B3']).rename('ndvi');
  return input.addBands(nd);
}

var L5_collection = ee.ImageCollection("LANDSAT/LT05/C01/T1_TOA")
  .filterBounds(geometry)
  .filterDate('2000-01-01', '2000-12-31')
  .filter(ee.Filter.lt("CLOUD_COVER", 0.1))
  .map(addndl5);

print(L5_collection);

var L5_mosaic = L5_collection.median().clip(geometry);

Map.addLayer(L5_mosaic, L5_display, "Landsat 5",false);

var ndvi_L5 = L5_collection.select('ndvi').median().clip(geometry);

Map.addLayer(ndvi_L5, {min: -0.1, max: 1, palette: ndvi_palette}, 'NDVI L5')

Map.centerObject(geometry);
Export.image.toDrive({
  image: ndvi_L5,
  description: 'NDVI_Landsat-2000',
  fileNamePrefix: 'NDVI_L5_',
  folder: 'Bhawalpurr',
  scale: 30,
  maxPixels: 1e13,
  region: geometry
```

Figure 3.3 Code of NDVI.

3.4.2.3 NDWI

NDWI stands for "Normalized Difference Water Index". It is a remote sensing index that is commonly used to detect the presence of water in an area using satellite imagery.

The NDWI index is calculated using the formula:

NDWI = (Green - NIR) / (Green + NIR) (Equation 3. 3)

Where, Green is the reflectance value in the green spectral band, and NIR is the reflectance value in the near-infrared spectral band.

The index ranges from -1 to 1, with values closer to 1 indicating a higher presence of water. Vegetation tends to absorb more of the green light, while the water reflects more of the near-infrared light, hence the use of these two spectral bands in the calculation of the index.

```
var ndwi_palette = 'FFFFFF, CE7E45, DF923D, F1B555, FCD163, 99B718, 74A901, 66A000,

//Landsat 5 (1984-2012)

var L5_display = {bands: ["B3", "B2", "B1"], min: 0, max: 0.5};

function addndl5(input) {
  var nd = input.normalizedDifference(['B5', 'B3']).rename('ndwi');
  return input.addBands(nd);
}

var L5_collection = ee.ImageCollection("LANDSAT/LT05/C01/T1_TOA")
  .filterBounds(geometry)
  .filterDate('1990-01-01', '1990-12-31')
  .filter(ee.Filter.lt("CLOUD_COVER", 0.1))
  .map(addndl5);

print(L5_collection);

var L5_mosaic = L5_collection.median().clip(geometry);

Map.addLayer(L5_mosaic, L5_display, "Landsat 5",false);

var ndwi_L5 = L5_collection.select('ndwi').median().clip(geometry);

Map.addLayer(ndwi_L5, {min: -0.1, max: 1, palette: ndwi_palette}, 'NDWI L5');
Map.centerObject(geometry);

Export.image.toDrive({
  image: ndwi_L5,
  description: 'NDWI_Landsat-5',
  fileNamePrefix: 'NDWI_L5_',
  folder: 'Bhawalpurr',
  scale: 30,
  maxPixels: 1e13,
  region: geometry
});
```

Figure 3.4 Code for NDWI.

3.4.2.4 LST

"Land Surface Temperature" is the abbreviation of LST. It is the temperature of the land surface as determined by a satellite or other remote sensing device[45].

The thermal behavior of the Earth's surface can be seen by the LST and is impacted by a number of variables, including solar radiation, cloud cover, and the presence of water or vegetation. Depending on the time of day, season, and weather, the LST might change significantly. Typically, thermal infrared sensors on board satellites are used to measure LST. These sensors pick up the infrared radiation, which is proportional to the surface temperature that the Earth's surface emits. Algorithms that account for atmospheric factors such the presence of water vapor and aerosols, which can impact temperature observations, can be used to compute the LST.

```
Map.addLayer(pakistan,{},'pakistan');
Map.setCenter(69.896,30.625);

//MODIS Day-time temperature
var modisLSTD = MODIS_LST.select('LST_Day_1km')
.filterDate('2000-03-01', '2000-09-30'); //selected date

//Converting Temperature from Kelvin to Celsius
modisLSTD = modisLSTD.map(function(image){
  return image.multiply(0.02).subtract(273.15).copyProperties(image, ['system:time_start']);
});

//Chart titles
var title = {
  title: 'Day Temperature',
  hAxis: {title: 'Time'},
  vAxis: {title: 'Temperature C'},
};

//Chart for day time temperature
var chart = ui.Chart.image.series
(modisLSTD,pakistan, ee.Reducer.mean(), 1000,'system:time_start')
    .setOptions(title)
    .setChartType('ColumnChart');
print('Day Surface Temperature in Celsius');
print(chart);

//Add LST layer in GEE
var landSurfaceTemperatureVis = {
  min: 0,
  max: 69,
  palette: [
    '040274', '040281', '0502a3', '0502b8', '0502ce', '0502e6',
    '0602ff', '235cb1', '307ef3', '269db1', '30c8e2', '32d3ef',
    '3be285', '3ff38f', '86e26f', '3ae237', 'b5e22e', 'd6e21f',
    'fff705', 'ffd611', 'ffb613', 'ff8b13', 'ff6e08', 'ff500d',
    'ff0000', 'de0101', 'c21301', 'a71001', '911003'
  ],
};
```

Figure 3.5 Code of LST.

Utilizing the thermal infrared bands of Landsat 5 and Landsat 8 data allows for the estimation of Land Surface Temperature (LST). Despite differences in sensor properties and data processing, both satellites offer useful information for LST estimation.

The Thematic Mapper (TM) sensor on board Landsat 5, which was deployed in 1984, has a thermal infrared band (band 6) with a spatial resolution of 120 meters. In order to estimate LST, this band detects the thermal radiation that the Earth's surface emits. It's crucial to keep in mind that since Landsat 5 stopped collecting data in 2012, there may not be as many recent LST estimations available using this sensor.

The Operational Land Imager (OLI) and Thermal Infrared Sensor (TIRS) are with Landsat 8, which was launched in 2013. Two thermal bands—TIRS 1 (band 10) and TIRS 2 (band 11)—are part of the TIRS instrument. Compared to Landsat 5, these bands have a spatial resolution of 100 meters higher and offer more precise LST estimates. Since Landsat 8's TIRS bands are made to be radiometric-ally calibrated, they can give LST data for a variety of uses.

The formula for estimating Land Surface Temperature (LST) from Landsat 5 and Landsat 8 data involves using the thermal infrared bands and applying specific conversions. Here are the general equations commonly used for LST estimation:

LST Estimation for Landsat 5

(Thematic Mapper - TM):

$$\mathbf{LST = K_2 / \ln((K_1 / Radiance) + 1)} \qquad \textbf{(Equation 3. 4)}$$

Where:

LST: Land Surface Temperature in Kelvin

Radiance: Thermal Infrared Radiance values from Landsat 5 band 6

K_1 and K_2: Empirical constants derived from sensor calibration

LST Estimation for Landsat 8

(Operational Land Imager - OLI and Thermal Infrared Sensor - TIRS):

$$\mathbf{LST = K_2 / (\ln((K_1 / Radiance) + 1) + C_2)} \qquad \textbf{(Equation 3. 5)}$$

Where:

LST: Land Surface Temperature in Kelvin

Radiance: Thermal Infrared Radiance values from Landsat 8 band 10 (TIRS 1) or band 11 (TIRS 2)

K_1 and K_2: Empirical constants derived from sensor calibration, specific to Landsat 8 TIRS

C_2: Offset constant accounting for atmospheric effects, also provided in the metadata

Similar to Landsat 5, the values of K_1, K_2, and C_2 for Landsat 8 are specific to the TIRS bands and can be obtained from the USGS or NASA.

3.4.2.5 Population Density

The World Bank estimates Pakistan's population density to be 287/km², as of 2021. It is crucial to remember that population density can change significantly between various provinces and areas within a nation. In Pakistan, it is the cities that have the largest population density, particularly Punjab and the Karachi metropolitan area. On the other hand, population densities are generally lower in rural areas. As a result of growing urbanization, the temperature in metropolitan areas increases.

```
var collection1 = ee.ImageCollection("CIESIN/GPWv411/GPW_Population_Density")
 var raster = collection1.select('population_density')
.filterDate('2020-04-01','2020-09-30');
var collection2 = ee.ImageCollection("CIESIN/GPWv411/GPW_Population_Density")
 var raster = collection2.select('population_density')
.filterDate('2021-04-01','2021-09-30');
var collection3 = ee.ImageCollection("CIESIN/GPWv411/GPW_Population_Density")
 var raster = collection3.select('population_density')
.filterDate('2019-04-01','2019-09-30');
var collection4 = ee.ImageCollection("CIESIN/GPWv411/GPW_Population_Density")
 var raster = collection4.select('population_density')
.filterDate('2015-04-01','2015-09-30');
var collection5 = ee.ImageCollection("CIESIN/GPWv411/GPW_Population_Density")
 var raster = collection5.select('population_density')
.filterDate('2010-04-01','2010-09-30');
var collection6 = ee.ImageCollection("CIESIN/GPWv411/GPW_Population_Density")
 var raster = collection6.select('population_density')
.filterDate('2005-04-01','2005-09-30');
var collection7 = ee.ImageCollection("CIESIN/GPWv411/GPW_Population_Density")
 var raster = collection7.select('population_density')
.filterDate('2000-04-01','2000-09-30');
Map.centerObject(geometry);
var raster_vis = {
  "max": 10000.0,
  "palette": [
    "ffffe7",
    "FFc869",
    "ffac1d",
    "e17735",
    "f2552c",
    "9f0c21"
  ],
  "min": 0.0
};
var PM2_5_2020 =  collection1.mean().clip(geometry);
var PM2_5_2021 =  collection2.mean().clip(geometry);
var PM2_5_2019 =  collection3.mean().clip(geometry);
var PM2_5_2015 =  collection4.mean().clip(geometry);
var PM2_5_2010 =  collection5.mean().clip(geometry);
var PM2_5_2005 =  collection6.mean().clip(geometry);
```

Figure 3.6 Code of Population Density.

3.4.2.6 PM2.5

PM2.5 is an abbreviation for "Particulate Matter 2.5". Small particles with a diameter of 2.5 micrometers or less make up this category of air pollution[46]. Dust, smoke, and chemicals released from machinery and industrial processes are just a few examples of the different materials that might make up these particles.

PM2.5 is especially worrisome since it can enter the bloodstream and travel deep into the lungs, causing a variety of health issues include cardiovascular and respiratory disorders. The World Health Organization (WHO) has defined standards for PM2.5 concentrations, with a daily mean of 25 g/m3 and an annual mean of 10 g/m3 over which it is deemed hazardous to human health.

Air quality monitoring stations measure the quantity of PM2.5 in the air and keep track of it. Policymakers use this information to decide on how to reduce air pollution, and people use it to protect their health by taking precautions like wearing masks or staying indoors during times of heavy pollution.

```
var collection1 = ee.ImageCollection('MODIS/006/MCD19A2_GRANULES')
                  .select('Optical_Depth_055')
                  .filterDate('2018-04-01', '2018-09-30');
var collection2 = ee.ImageCollection('MODIS/006/MCD19A2_GRANULES')
                  .select('Optical_Depth_055')
                  .filterDate('2019-04-01', '2019-09-30');
var collection3 = ee.ImageCollection('MODIS/006/MCD19A2_GRANULES')
                  .select('Optical_Depth_055')
                  .filterDate('2020-04-01', '2020-09-30');
var collection4 = ee.ImageCollection('MODIS/006/MCD19A2_GRANULES')
                  .select('Optical_Depth_055')
                  .filterDate('2021-04-01', '2021-09-30');
var collection5 = ee.ImageCollection('MODIS/006/MCD19A2_GRANULES')
                  .select('Optical_Depth_055')
                  .filterDate('2000-04-01', '2000-09-30');
var collection6 = ee.ImageCollection('MODIS/006/MCD19A2_GRANULES')
                  .select('Optical_Depth_055')
                  .filterDate('2005-04-01', '2005-09-30');
var collection7 = ee.ImageCollection('MODIS/006/MCD19A2_GRANULES')
                  .select('Optical_Depth_055')
                  .filterDate('2010-04-01', '2010-09-30');
var collection8 = ee.ImageCollection('MODIS/006/MCD19A2_GRANULES')
                  .select('Optical_Depth_055')
                  .filterDate('2015-04-01', '2015-09-30');
Map.centerObject(geometry);
var band_viz = {
  min: 329.9166666666667,
  max: 703.75864,
  palette: ['black', 'blue', 'purple', 'cyan', 'green', 'yellow', 'red']
};
var PM2_5_2018 =  collection1.mean().clip(geometry);
var PM2_5_2019 =  collection2.mean().clip(geometry);
var PM2_5_2020 =  collection3.mean().clip(geometry);
var PM2_5_2021 =  collection4.mean().clip(geometry);
var PM2_5_2000 =  collection5.mean().clip(geometry);
var PM2_5_2005 =  collection6.mean().clip(geometry);
var PM2_5_2010 =  collection7.mean().clip(geometry);
var PM2_5_2015 =  collection8.mean().clip(geometry);
Map.addLayer(PM2_5_2018, band_viz, 'PM2_5_2018');
Map.addLayer(PM2_5_2019, band_viz, 'PM2_5_2019');
Map.addLayer(PM2_5_2020, band_viz, 'PM2_5_2020.5');
```

Figure 3.7 Code for PM2.5.

3.5 Determination of LULC Area

Land Use and Land Cover, or LULC, is an abbreviation for the physical and biological characteristics of the Earth's surface. The term "land use" describes how people use the land, such as for agriculture, habitation, commerce, industry, or enjoyment. The physical surface cover of the land, such as woods, meadows, water bodies, bare soil, or urban areas, is referred to as land cover[47]. A region's social, economic, and environmental characteristics are greatly influenced by LULC. Climate, biodiversity, water resources, agricultural production, human health, and other ecological and social systems can all be significantly impacted by changes in LULC. Therefore, for sustainable land use planning and management, monitoring and managing LULC patterns and changes is crucial.

Different techniques, such as remote sensing, field surveys, and GIS analysis, can be used to calculate Land Use and Land Cover (LULC)[48]. A popular technique for determining LULC is remote sensing, which uses satellite or aerial photography to identify and map various land use and land cover categories. Many sources, like Landsat, MODIS, and Sentinel, which offer high-resolution satellite images at multiple spectral bands, can be used to collect remote sensing data. The process of LULC determination through remote sensing typically involves the following steps:

1. **Image acquisition:**

   Obtain satellite images of the area of interest. We have obtained our desired areas of Multan, Lahore, Rawalpindi and Faisalabad of year 2000 and 2020 from USGS.

2. **Image preprocessing:**

   The satellite images are preprocessed to remove distortions and enhance the image quality. This step includes radiometric and atmospheric corrections to adjust for differences in the lighting and atmospheric conditions during image acquisition.

3. **Image classification:**

   This step involves the identification and classification of different land cover types in satellite imagery. Supervised and unsupervised classification methods are commonly used for this step. Supervised classification involves the manual selection of training samples, which are then used to classify the entire image. Unsupervised classification, on the other hand, uses clustering algorithms to group similar pixels into classes.

4. **Accuracy assessment:**

The accuracy of the classification results is assessed by comparing the classified image with ground truth data obtained through field surveys or other validation methods.

5. LULC mapping:

The final step involves generating LULC maps that show the different land use and land cover types in the area of interest[49].

We have used Arc-GIS software interpretation and mapping of LULC area for our desired cities.

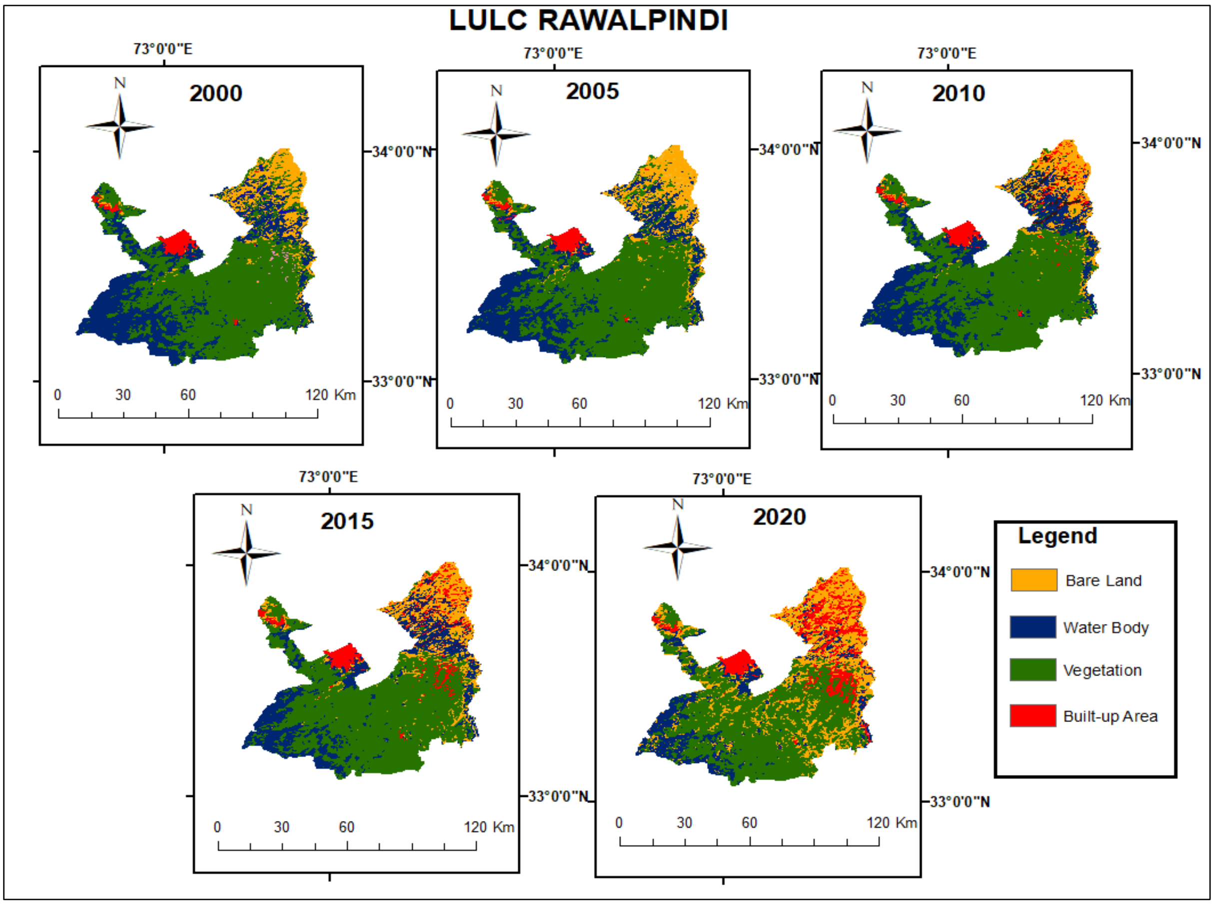

Figure 3.8 LULC map for Multan city for year 2000 to 2020.

3.5.2 Classes of LULC

The classes used in mapping of LULC data are as follow[31]:

<u>Built-Up Area</u>

This class represents areas characterized by high-density human development, including residential, commercial, industrial, and infrastructure areas.

Vegetation Area

This class encompasses various types of natural vegetation, including forests, woodlands, grasslands, shrub-lands, and wetlands.

Water Bodies

This class represents different types of water bodies, including rivers, lakes, reservoirs, ponds, and oceans.

Bare Land

This class refers to areas devoid of vegetation cover, typically including exposed soil, barren land, and rocky surfaces.

3.5.3 Accuracy Assessment

A statistical indicator of agreement or dependability between two sets of data is the kappa coefficient. The accuracy of land use and land cover (LULC) maps created by remote sensing analysis is frequently evaluated in image classification and remote sensing investigations[50].

The kappa coefficient measures the observed agreement between a reference data set, often obtained by ground truth or other validation techniques, and a LULC map produced through remote sensing analysis. The coefficient corrects for the degree of agreement that may be anticipated by chance and takes into account both the number of correct classifications and the number of incorrect classifications made by the remote sensing study. The scale goes from -1 to 1, where 1 denotes perfect agreement, 0 denotes agreement no better than chance, and negative numbers denote disagreement worse than chance. The LULC map and the reference data set are typically thought to have a high level of agreement or correctness if the kappa coefficient is 0.8 or above.

The kappa coefficient can be used to direct future data collection and analysis in order to enhance the accuracy of the maps. It is a useful tool for assessing the correctness of LULC maps produced using remote sensing analysis.

3.5.4 Confusion Matrix

A helpful tool for evaluating the precision of Land Use/Land Cover (LULC) classifications is the Confusion Matrix. It assesses the degree of agreement and discrepancy between the observed LULC classes and the categorized classes[51]. By calculating the degree of agreement between the classified and reference data, the Confusion Matrix feature in ArcGIS enables you to evaluate the accuracy and dependability of your LULC classification findings. It aids in understanding the benefits and drawbacks of your classification and reveals any potential areas for development.

Table 3.2 Confusion Matrix of Multan for the year 2000.

OBJECTID	Class Value	Water body	Vegetation	Built-up	Bare land	Total	U-Accuracy	Kappa
1	Water body	2	0	0	0	2	1	0
2	Vegetation	1	69	0	0	70	0.985714	0
3	Built-up	1	3	19	0	23	0.826087	0
4	Bare land	0	0	0	1	1	1	0
5	Total	4	72	20	1	100	0	0
6	P-Accuracy	0.5	0.958333	0.95	1	0	0.94	0
7	Kappa	0	0	0	0	0	0	**0.866042**

3.5.5 Kappa co-efficient formula and accuracy of kappa values

The Kappa coefficient, commonly referred to as Cohen's kappa, is a statistical metric used to determine whether two raters or classifiers agree on the category labels or ratings they should assign. It accounts for both the observed and the expected by chance levels of agreement. The formula for calculating Cohen's kappa coefficient is as follows:

$$\kappa = \frac{p_0 - p_e}{1 - p_e}, \qquad \textbf{(Equation 3. 6)}$$

Where:

- K represents Cohen's kappa coefficient.
- P_o is the observed agreement, which is the proportion of cases where both raters agree.
- P_e is the expected agreement, which is the proportion of cases where agreement is expected by chance.

The kappa coefficient ranges from -1 to 1, where a value of 1 indicates perfect agreement, 0 indicates agreement by chance, and -1 indicates complete disagreement.

- Values less than 0: Indicates less agreement than would be expected by chance. There is a significant disagreement between the raters or classifiers.

- Values between 0 and 0.20: Indicates slight agreement beyond chance.
- Values between 0.21 and 0.40: Indicates fair agreement.
- Values between 0.41 and 0.60: Indicates moderate agreement.
- Values between 0.61 and 0.80: Indicates substantial agreement.
- Values between 0.81 and 1: Indicates almost perfect agreement[52].

3.6 Parameters used for Urban Growth Modeling

Predicting the spatial and temporal patterns of urban expansion is the goal of urban growth modeling. Urban growth models take into account a number of variables and elements to accurately depict the complex dynamics of urban development[53]. Here are some parameters that are frequently used in urban growth modeling:

Land Use/Land Cover (LULC) Data

The types of land cover and existing urban areas are revealed by historical LULC data. The urban growth model may be calibrated and validated using this data.

Socioeconomic Factors

Urban growth is influenced by socioeconomic factors such as population growth, economic indicators (such as GDP), employment rates, and migration trends. These factors aid in capturing the need for urban growth and serve as a guide for future growth estimates.

Infrastructure and Accessibility

Urban expansion may be influenced by the availability of infrastructure, such as road networks, transportation networks, and utility services. The patterns of expansion are influenced by accessibility factors, such as proximity to highways or distance from transportation hubs.

Environmental Factors

Urban growth may be impacted by environmental factors such as topography, slope, the appropriateness of the soil, water bodies, and biological limitations. These variables aid in separating out locations with limitations or vulnerabilities from those that are appropriate for development.

Zoning and Land Use Policies

Urban growth patterns are influenced by zoning laws and land use rules implemented by municipal governments. These regulations may limit or encourage development in particular locations, affecting the extent and pace of urbanization.

Spatial Interactions and Spatial Metrics

The impact of nearby urban centers on the development of a specific location is taken into account by spatial interaction models. Urban growth's spatial characteristics are quantified by spatial metrics including fragmentation indices, compactness measurements, and proximity analysis, which also aid in assessing the effects of urban growth.

Machine Learning and Statistical Techniques

Based on the input parameters, urban expansion is simulated and predicted using a variety of machine learning algorithms and statistical techniques, such as regression models, cellular automata, and agent-based models. These techniques enable the creation of prediction models by capturing the intricate interactions between variables.

Calibration and Validation Data

For evaluating the precision and effectiveness of the urban growth model, calibration and validation data are crucial. The model is calibrated using historical growth trends, satellite images, and real-world data, and then validated using independent datasets.

3.7 Visualization of data on Arc GIS

Depending on the type of data and the desired visualization, there are various ways to visualize data on ArcGIS. We've employed one of the most popular methods for visualizing data on ArcGIS is by adding point, line, or polygon data to a map. To accomplish this, import the shape-files from GIS Pakistan into ArcGIS and symbolize the data using various variables like size, color, and shape.

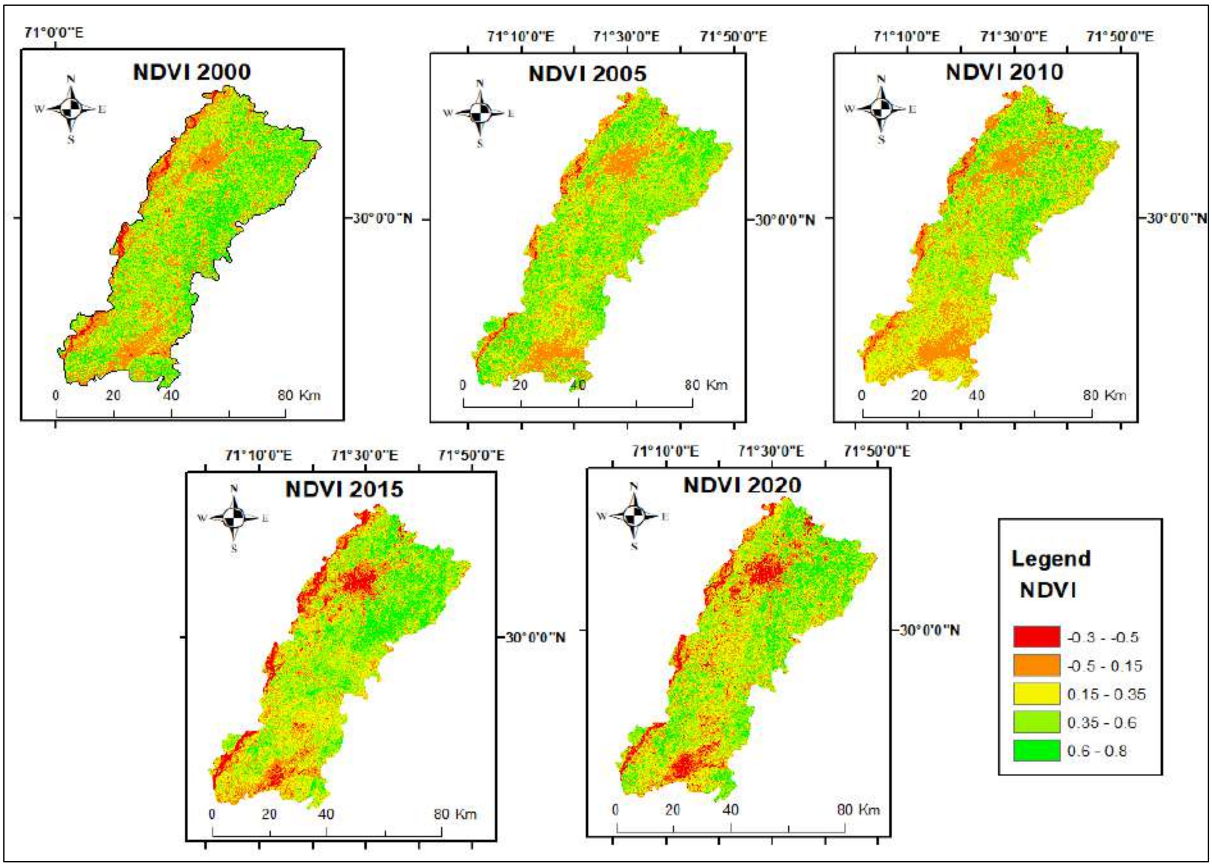

Figure 3.9 Mapping of NDVI for District Multan.

3.8 Artificial Neural Network (ANN)

Computer models called Artificial Neural Networks (ANNs) are modeled after the structure and operation of organic neural networks, including the human brain. An essential part of machine learning, ANNs are intended to identify intricate patterns, forecast the future, and resolve a variety of issues[54]. They are made up of layers of interconnected artificial neurons that process information by varying connection weights. An input layer, one or more hidden layers, and an output layer are the layers that make up an ANN. Data is received by the input layer, where it is processed and changed before moving through the hidden levels. Each artificial neuron generates an output after applying a mathematical function to its inputs using weights and biases[55]. Up until the final output is generated, the outputs from one layer are used as the inputs for the subsequent layer.

The weights and biases of ANNs are changed as they learn in order to reduce the discrepancy between projected and actual results. This is accomplished through a training step, usually utilizing the back propagation technique. In order to change the link weights and biases, back propagation computes the difference between predicted and expected outputs and propagates that difference backward through the network. Until the network reaches a desired level of performance, this iterative process is continued. ANNs can recognize intricate patterns and connections in data, which makes them particularly adept at jobs like speech and picture recognition, natural language processing, time series prediction, and classification issues. Deep Neural Networks (DNNs), which are ANNs with many hidden layers, have excelled in achieving cutting-edge performance across a variety of domains. Advancements in areas like computer vision, autonomous driving, and language translation have been made thanks to DNNs[56].

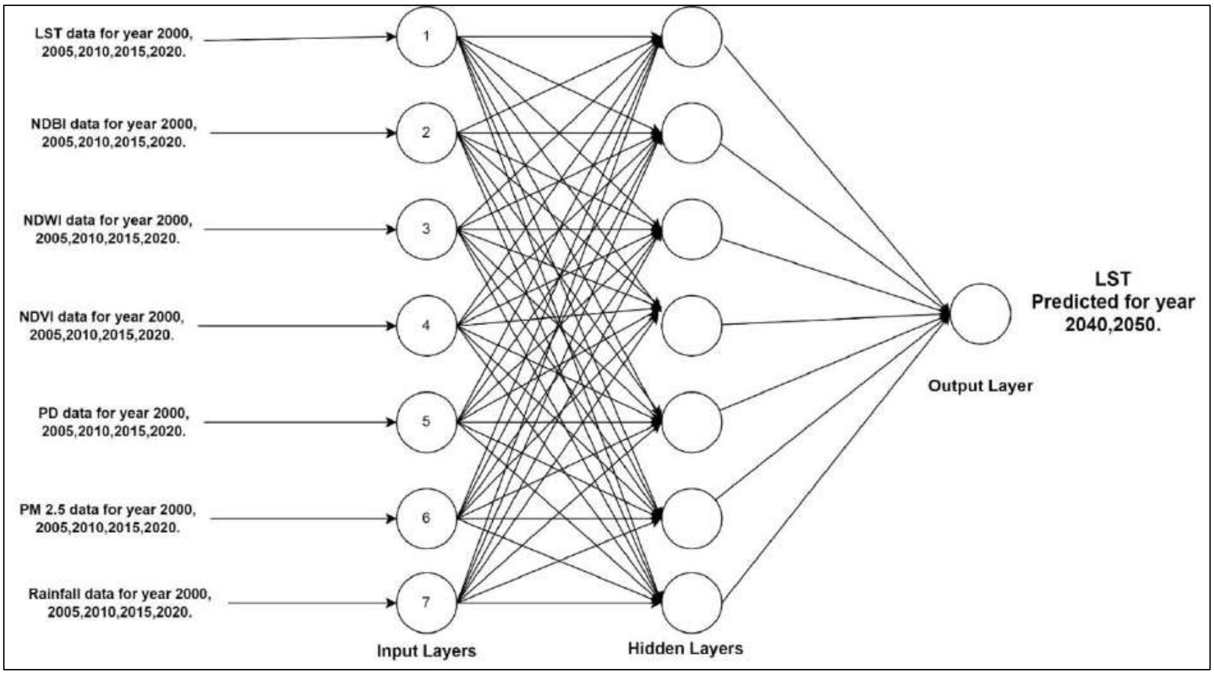

Figure 3.10 Model for ANN.

3.9 Mitigation

Instead of directly addressing climate change, we have conducted mitigation using the ENVI-met software, which largely focuses on micro-climatic modeling. Envi-Met can simulate and evaluate various UHI mitigation techniques, including cool pavements, cool roofs, and shade structures. Envi-Met assists in putting policies in place that lessen the local climate impact and indirectly support broader climate change mitigation by analyzing the efficacy of these interventions in reducing UHI intensity[57]. It can be used to evaluate and improve the energy efficiency of structures and urban systems. Envi-Met helps detect high energy usage areas by modeling energy consumption, such as heat gain through building envelopes or ineffective cooling systems. This knowledge can direct efforts to increase energy efficiency, lower carbon emissions, and combat climate change.

3.10 Simulation

We have done Simulation on ENVI-met software and the procedure involves is as follow[57]:

Project Setup

Setting up the simulation project in Envi-Met is the initial stage. The geographic area of interest must be specified, the digital terrain model (DTM) must be imported or created, and the local meteorological information must be specified.

Designing the Urban Environment

By including structures, streets, parks, and other urban characteristics, Envi-Met offers tools for designing the urban environment. 3D models of buildings can be imported or created, and their shape, materials, and attributes like thermal conductivity and reflection can all be changed.

Vegetation and Land Cover

Different kinds of vegetation and land cover can be included in Envi-Met. To replicate the cooling and shading benefits of vegetation, you can include trees, grass, shrubs, and other plant features. To match actual conditions, parameters like leaf area index, canopy cover, and photosynthetic rates can be changed.

Meteorological Inputs

For Envi-Met to simulate weather conditions, meteorological inputs are necessary. Meteorological information can be entered, including air temperature, wind speed, humidity, and sun radiation. Local weather stations or meteorological databases can provide this data.

Running the Simulation:

Envi-Met can be used to start the simulation once all required inputs have been defined. The program uses computational techniques to mimic how structures, vegetation, and the atmosphere interact. Within the modeled area, it computes many factors like temperature, humidity, wind velocity, and solar radiation dispersion.

Simulation Output and Analysis

Envi-Met produces output data and visualization tools to assess the results after the simulation is complete. Maps of the temperature, wind patterns, and other pertinent characteristics can be seen. For additional investigation, the software offers quantitative information such as heat balance calculations, radiation fluxes, and temperature profiles.

Scenario Testing and Optimization

Envi-Met enables scenario testing and environmental and urban design factor optimization. To test their effects on the microclimate, you can change variables like surface materials, vegetation species, and building orientation. This iterative method aids in optimizing design decisions to attain desired results, such lowering the effects of urban heat islands or enhancing thermal comfort.

Validation and Calibration

To assure the accuracy and dependability of the simulation findings in Envi-Met, validation and calibration are crucial. This entails comparing the simulated results with actual measurements and making any necessary corrections.

3.11 Prediction

A large dataset and a trained model are necessary for predicting changes in Land Surface Temperature (LST) and Land Use and Land Cover (LULC) for upcoming years using Artificial Neural Networks (ANN)[58]. Here is a general description of what happens:

Data Collection

Collect past data on LST and LULC for the study area, spanning a time frame up to the present. This information ought to include elements like historical temperature data, satellite images, and descriptions of the types of land cover. Additionally, gather pertinent environmental and socioeconomic data that could affect future developments.

Data Preprocessing

The gathered data should be cleaned and prepared. To maintain consistency and compatibility for training the ANN model, this entails deleting outliers, filling in blanks, and standardizing the data.

Feature Selection

Determine the elements (such as climate variables, types of land cover, and demographics) that have the greatest impact on LST and LULC fluctuations. Techniques for feature selection, including correlation analysis or statistical testing, can be used to find relevant predictors.

Training the ANN Model

Create training and validation sets from the preprocessed data. To train the ANN model, use the training set. Through experimentation and validation, the ANN's design and parameters, including the number of layers, neurons, and activation functions, should be tuned. The link between the input characteristics and the goal variables (LST and LULC) should be taught to the model.

Model Validation

Using the validation dataset, evaluate the trained ANN model's performance. To gauge the precision of the predictions, look at measures like mean squared error (MSE), root mean square error (RMSE), or R-squared.

Future Data Preparation

Gather information for the predictors (such as projected changes in the climate, population growth, and land use regulations) for the years 2040 and 2050. Make sure the data are in the same format and range as those used for model training.

Prediction

Utilize the prepared future data to predict LST and LULC for the years 2040 and 2050 using the trained and validated ANN model. Based on the input predictors, the model ought to offer projected values or classifications for LST and LULC.

Result Analysis

To detect and interpret the anticipated changes and trends in the research area for the given years, analyze the predicted LST and LULC maps or values. This research can aid in planning for future land management and urban development plans by assisting stakeholders and decision-makers in understanding potential implications.

Chapter 4

4.1 Introduction

Following a comprehensive discussion of the procedures that were followed during the process of this study, we will now turn our attention to the findings and the outcomes that were accomplished. This chapter includes the analysis and interpretation of the data that was collected, shedding light on the most important observations and trends that were seen during the duration of the study. By analyzing the results that were acquired, it will be possible to achieve a thorough understanding of the study aims and issues, which will, in the end, contribute to a greater body of knowledge in the area of study.

The results and discussion of this project are described in the following sub-section:

4.2 Lahore

4.2.1 LULC

Table 4.1 LULC data for district Lahore.

Years	Temperature(°C)	Builtup(%)	vegetation(%)	Water(%)	Bareland(%)
2000	51.79	22.99	53.21	1.66	22.14
2005	51.98	27.73	65.04	2.62	4.61
2010	54.15	39.06	55.6	1.28	4.06
2015	54.39	41.17	53.51	1.13	4.19
2020	56.33	43.17	53.16	1.77	1.9
2040	58.21	58.23	41.12	0.35	0.3
2050	59.21	63.34	35.92	0.45	0.29

From table 4.1, there is a clear correlation between the passage of time and the increase in temperature. As the built-up area has expanded from 22.99% to 63.34%, the temperature has risen from 51.79℃ to 59.21℃. Simultaneously, there has been a decrease in vegetation area from 53.21% to 35.92%, water body from 1.66% to 0.45%, and bareland from 22.14% to

0.29%. These changes in land cover percentages indicate a trend of urbanization and the subsequent impact on temperature, resulting in an overall temperature increase over the past years.

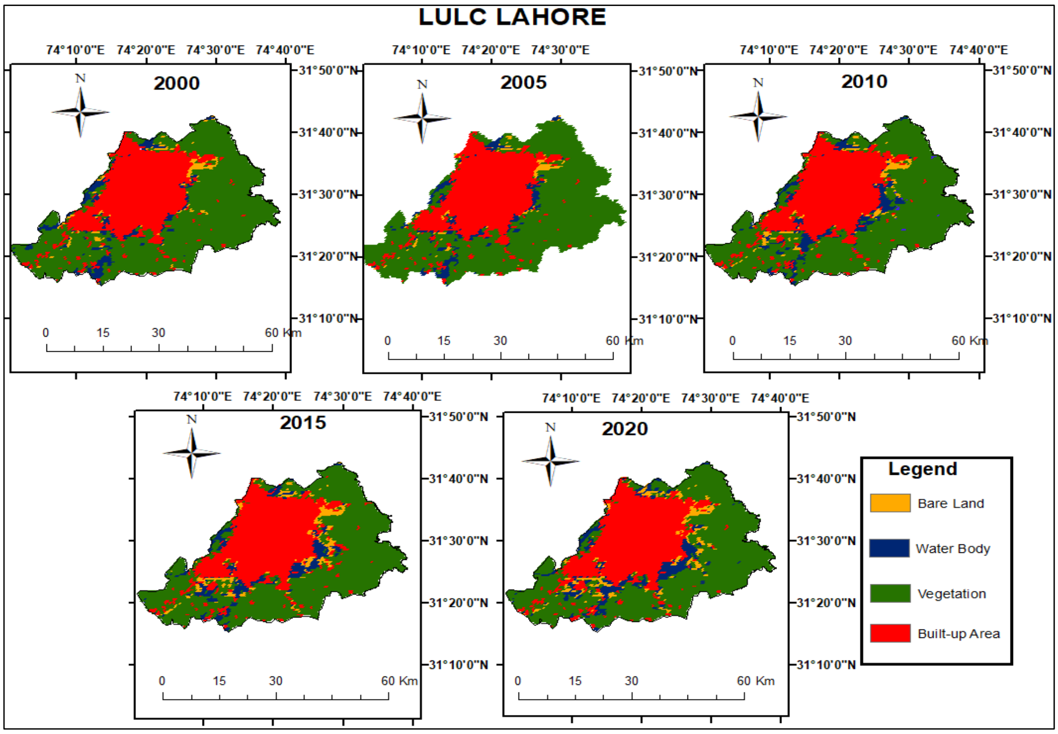

.

Figure 4.1 LULC of Lahore for year 2000 to 2020.

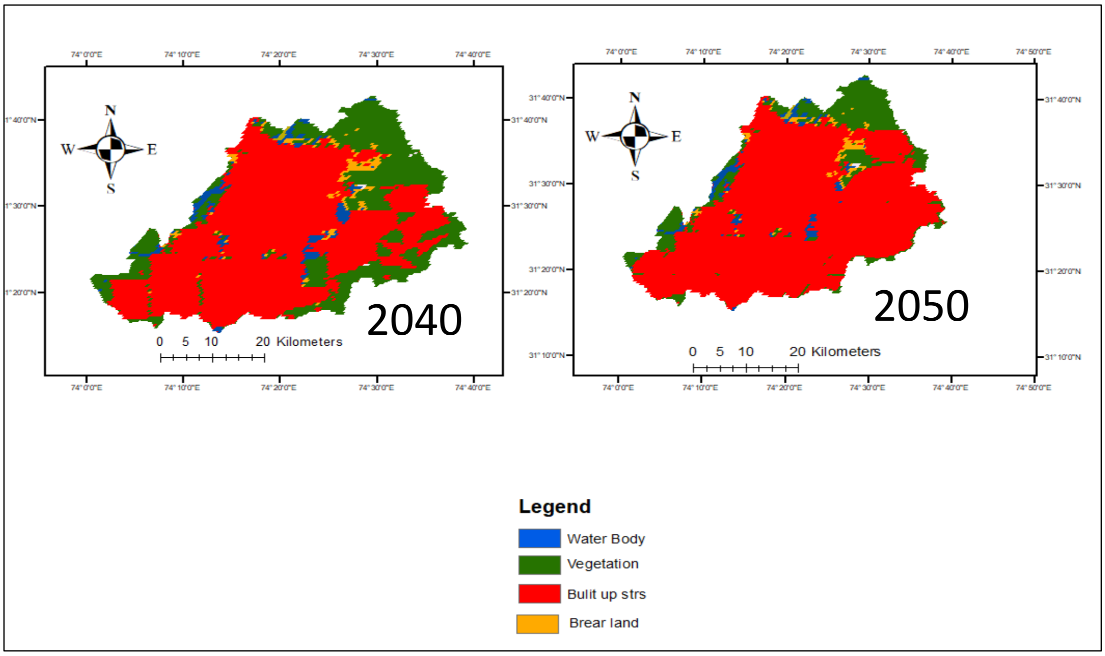

Figure 4.2 Predicted LULC for year 2040 and 2050 of Lahore.

As you can see in Figure 4.1, there is a increase in the built-up region in the middle of the map, which is actually a collection of towns arranged in a row.Due to its convenient position and strategic location in Lahore, Ravi Town has experienced significant urban expansion. A lot of built-up areas are there because it has become a popular location for residential and commercial buildings.Similar to this, the central Lahore neighbourhood of Data Gunj Baksh Town has seen tremendous urban expansion. It has drawn a variety of economic activity, including markets, shopping centres, and offices, making it a key and well-connected region, which has resulted in a sizable built-up area.In the northeastern region of Lahore, Samanabad Town has also witnessed significant urbanisation.As,we are progressing towards year 2050,the built-up area is increased around these towns as seen in Figure 4.2 as well.

4.2.2 LST

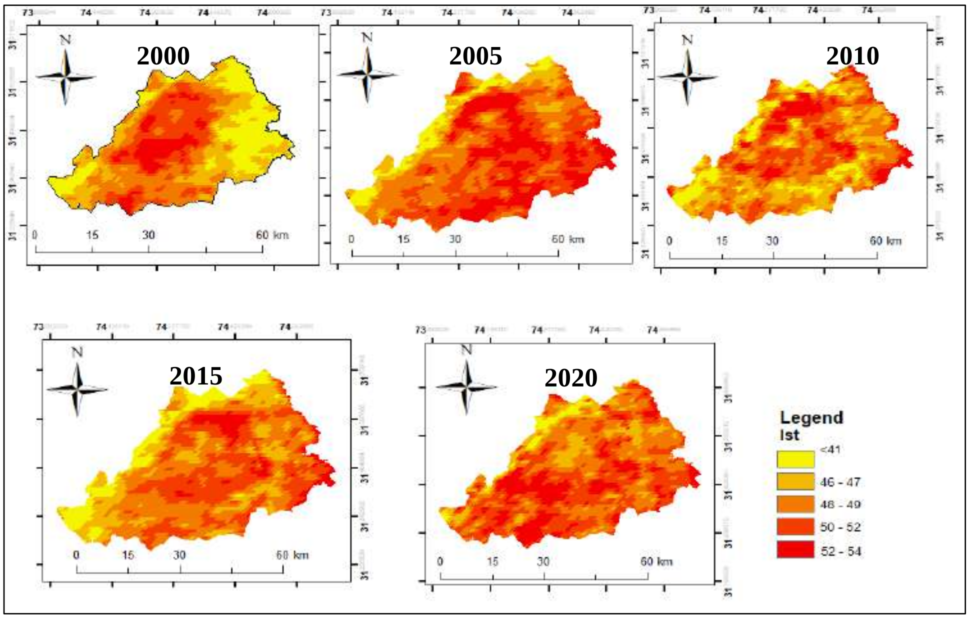

Figure 4.3 LST of Lahore for year 2000 to 2020.

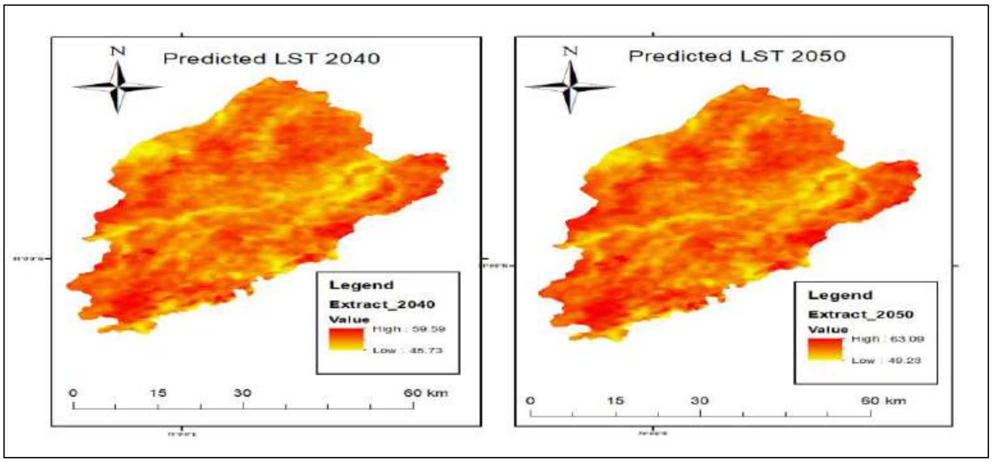

Figure 4.4 Predicted LST of Lahore for year 2040 and 2050.

As you can see in Figure 4.3 that the high Land Surface Temperature (LST) recorded in the Lahore District's Ravi Town, Data Gunj Baksh Town,Iqbal Town and Samanabad Town is increased as we are progressing towards year 2020.There are more structures, concrete, and asphalt surfaces here, which absorbs and holds heat, causing higher temperatures.The cooling impact of evapotranspiration and shade is diminished when there aren't any trees or green spaces. These communities also contribute to rising temperatures by emitting anthropogenic heat into the atmosphere through their industrial operations, vehicle emissions, and energy use. Additionally, the potential for evaporative cooling is diminished by the poor distribution of water bodies in these regions.The higher values of LST are observed in year 2050 as well as shown in Figure 4.4.

4.3 Rawalpindi

4.3.1 LULC

Table 4.2 LULC data for district Rawalpindi.

Years	Temperature(°C)	Builtup(%)	vegetation(%)	Water(%)	Bareland(%)
2000	51.81	9.4	89.1	1.2	0.3
2005	52.11	10.6	88.1	0.89	0.41
2010	55.23	10.5	88.5	0.58	0.42
2015	56.21	11.3	87.8	0.46	0.44
2020	57.41	12.8	86.3	0.45	0.45
2040	59.42	20.3	79	0.2	0.5
2050	61.21	25.69	73.5	0.1	0.91

From table 4.2, there is a clear correlation between the passage of time and the increase in temperature. As the built-up area has expanded from 9.4% to 25.69%, the land surface temperature has increased from 51.81°C to 61.21°C. Simultaneously, there has been a decrease in vegetation area from 89.1% to 73.5%, water body from 1.2% to 0.1%, and increase in bareland from 0.3% to 0.91%. These changes in land cover percentages indicate a trend of urbanization and the subsequent impact on temperature, resulting in an overall temperature increase over the past years.

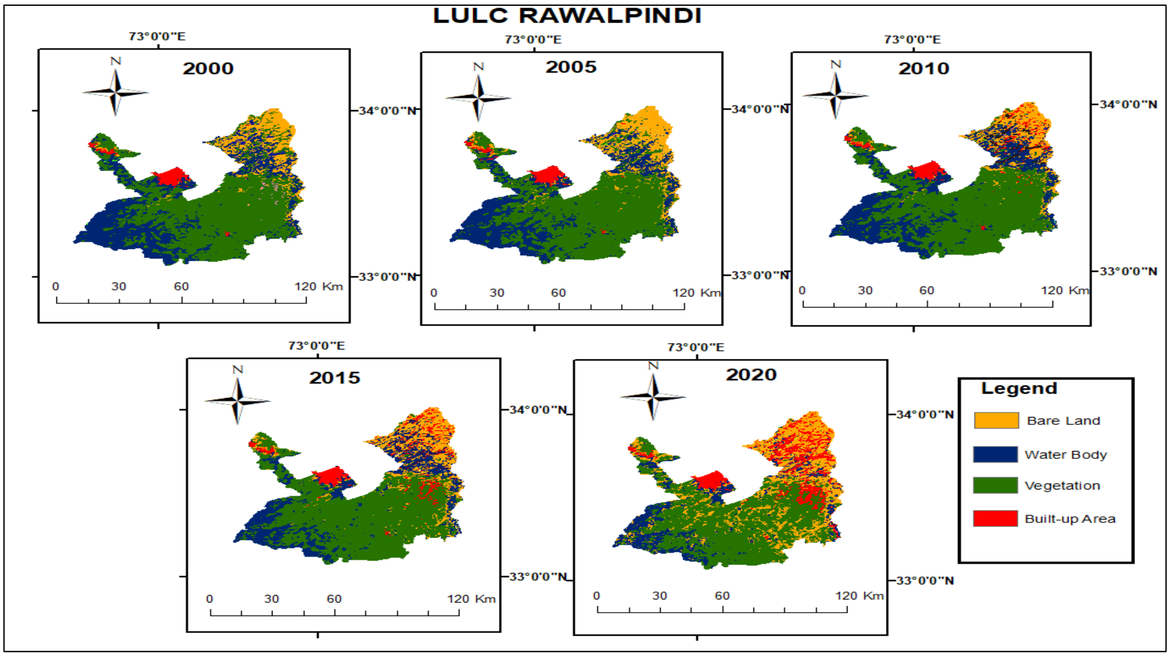

Figure 4.5 LULC of Rawalpindi for year 2000 to 2020.

.

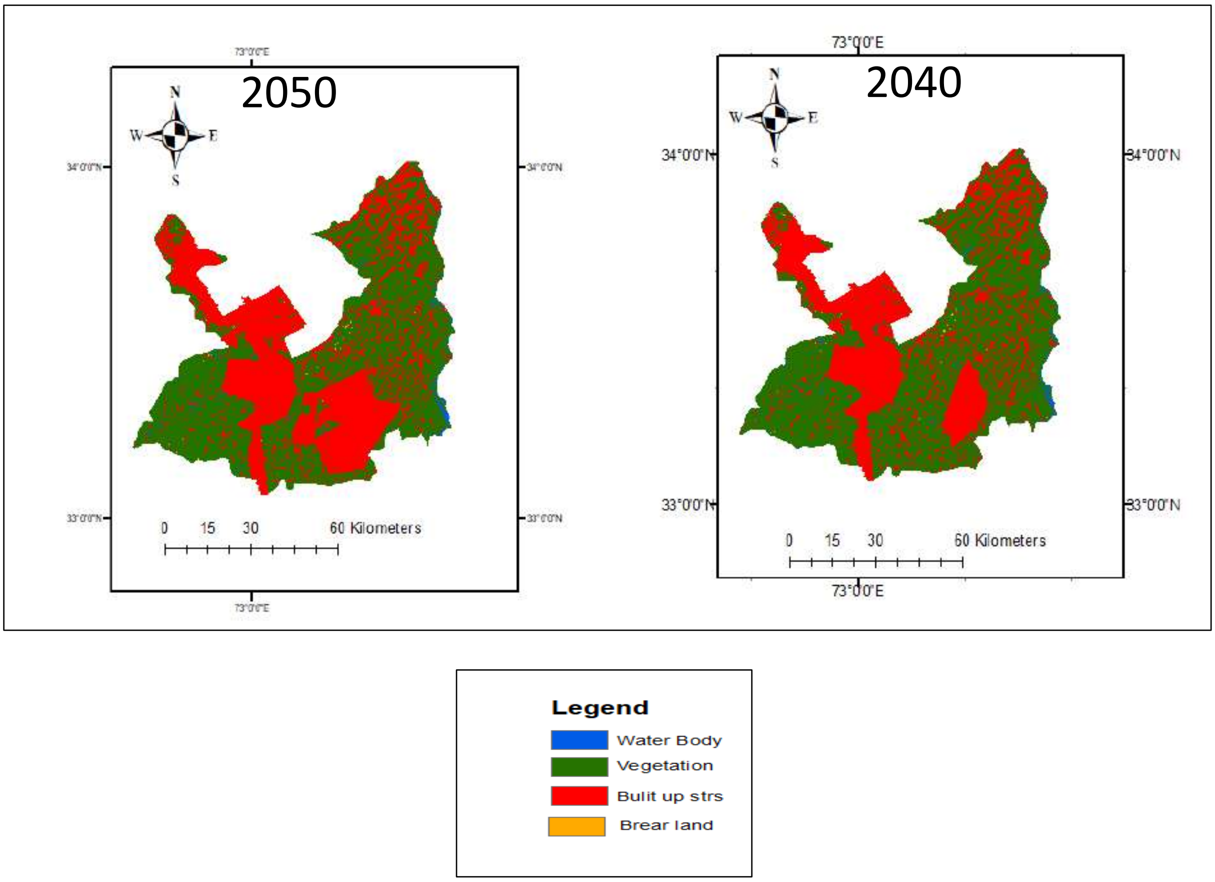

Figure 4.6 Predicted LULC of Rawalpindi for year 2040 and 2050.

As the primary hub for transport services, as shown in figure 4.5, the built-up area is rising in the Faizabad region of Rawalpindi. As a result, heat is created in Faizabad due to the regions high population density as well as expanding commercial and industrial activities. Energy use, transportation, and the presence of industrial facilities all contribute to the release of waste heat into the environment, which causes the LST to rise even higher. However, as we get closer to the year 2050, there is an increase in the built-up area in the Taxila and Gujjar Khan region, as well as as shown in Figure 4.6.

4.3.2 LST

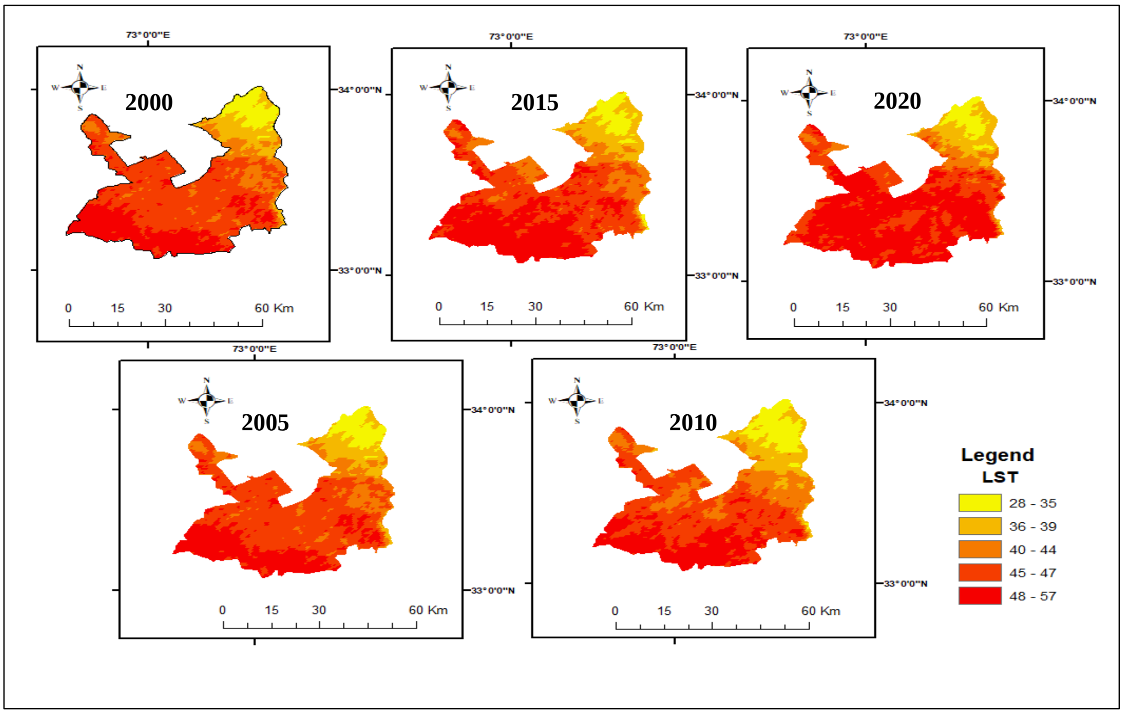

Figure 4.7 LST of Rawalpindi from year 2000 to 2020.

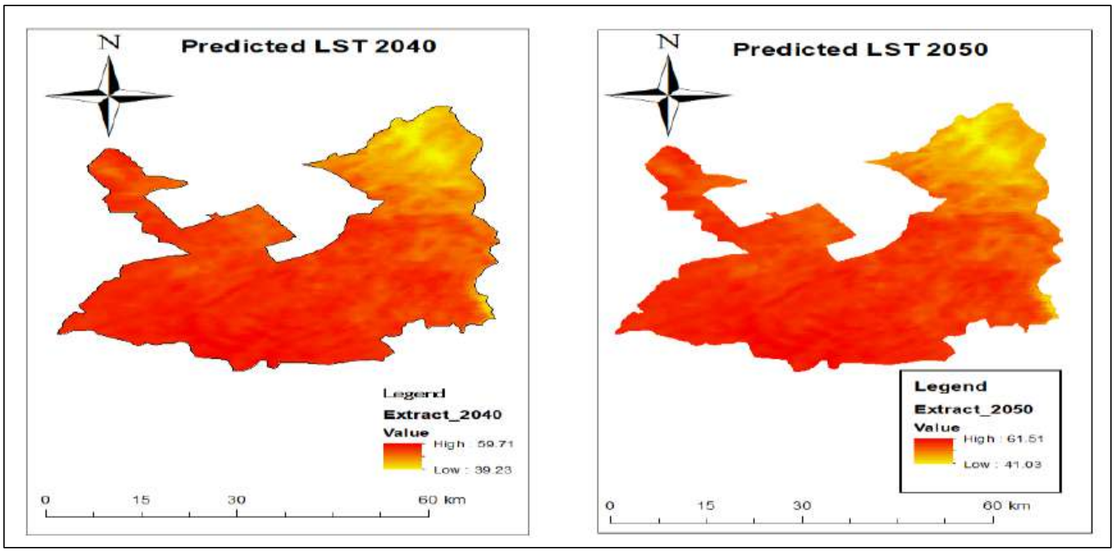

Figure 4.8 Predicted LST of Rawalpindi for year 2040 and 2050.

Figure 4.7 makes it visible that as we approach 2020, the LST has risen for the most of regions except Murree. Murree's elevation and topography are one important element. Due to its location near the mountains and greater altitude in the Margalla Hills, Murree enjoys cooler weather. Lower temperatures are caused by the thinner air that occurs as height rises. Additionally, the hilly landscape improves air circulation, which promotes heat dissipation and lowers LST. The amount of vegetation in Murree is a key factor in reducing LST. With a wide range of trees, bushes, and plants, the area is known for its deep woods and greenery as it is further observed in Figure 4.8 as well..

4.4 Multan

4.4.1 LULC

Table 4.3 LULC data for district Multan.

Years	Temperature(℃)	Builtup(%)	vegetation(%)	Water(%)	Bareland(%)
2000	55.65	10.4	85.8	2.4	1.4
2005	57.35	11.4	84.9	2.2	1.5
2010	58.11	12.9	83.7	1.9	1.5
2015	58.39	13.2	83.2	1.8	1.8
2020	60.78	15.3	81.9	1.1	1.7
2040	62.12	25.4	72.4	0.7	1.5
2050	64.21	28.7	69.4	0.6	1.3

From table 4.3, there is a positive correlation between the passage of time and the increase in land surface temperature. As the built-up area has expanded from 10.4% to 28.7%, the land surface temperature has increased from 51.81℃ to 61.21℃. Simultaneously, there has been a decrease in vegetation area from 85.8% to 69.4%, water body from 2.4% to 0.6%, and bareland from 1.4% to 1.3%. These changes in land cover percentages indicate a trend of urbanization and the subsequent impact on temperature, resulting in an overall temperature increase over the past years.

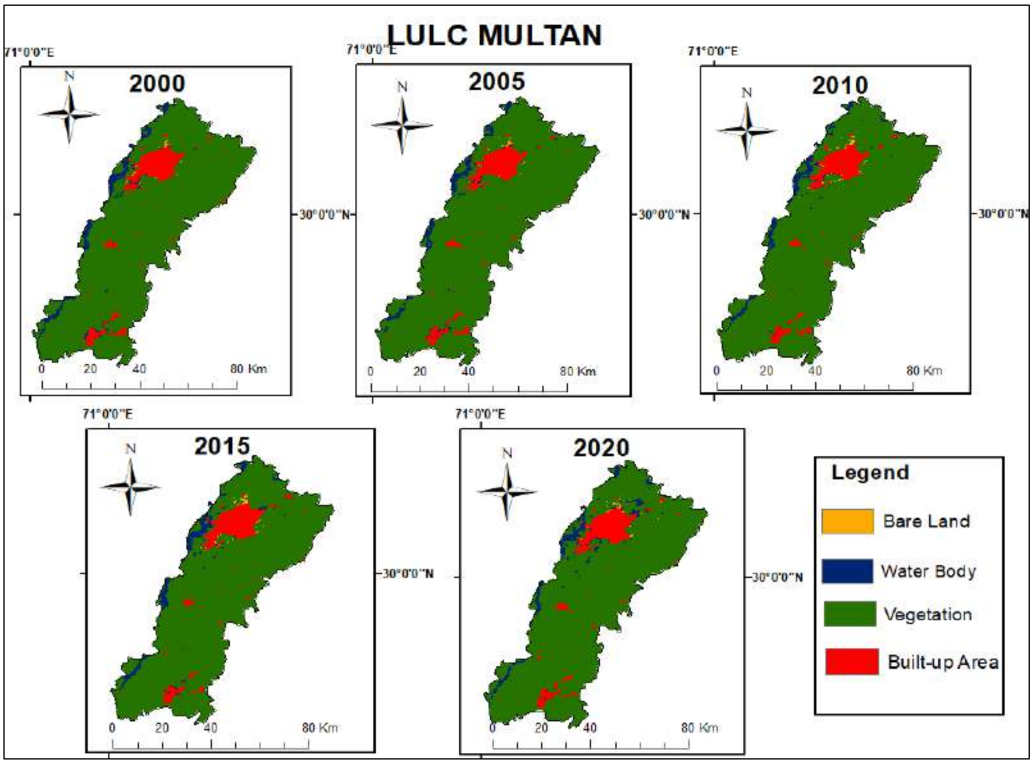

Figure 4.9 LULC of Multan for year 2000 to 2020.

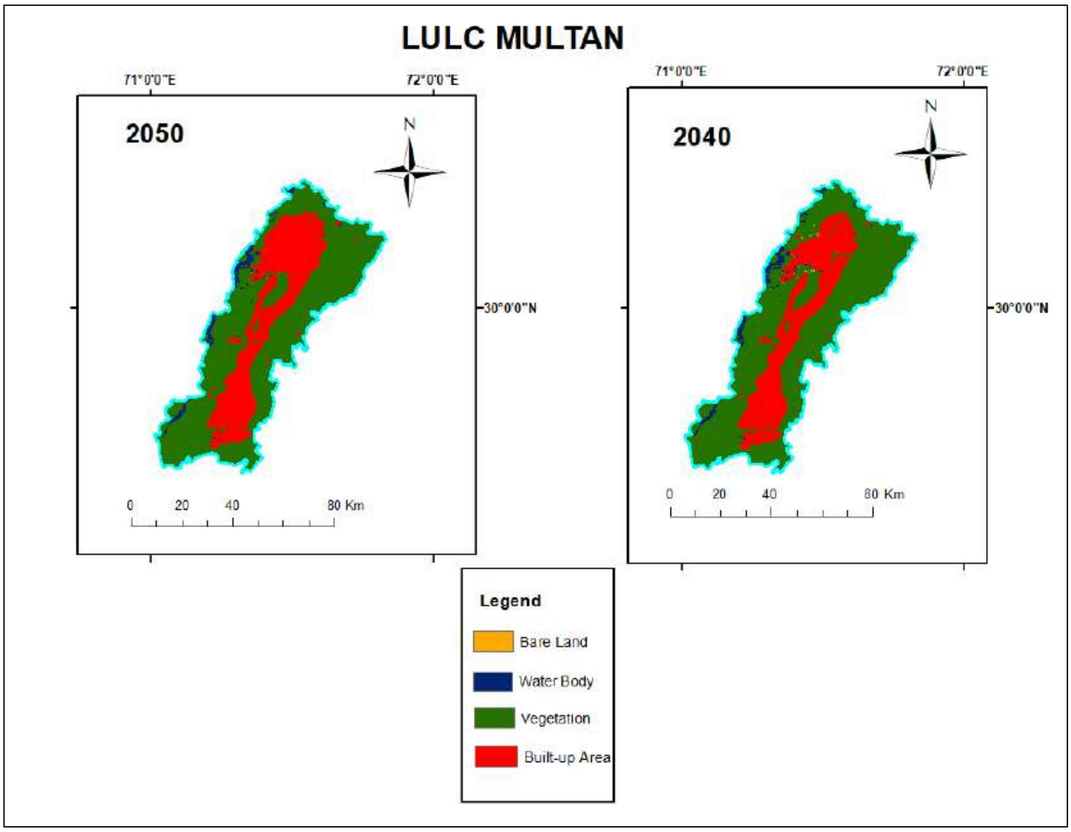

Figure4.10 Predicted LULC of Multan for year 2040 and 2050.

As you can see in figure 4.9 which shows that the built-up area is growing on the upper part of Multan District, which is actually an area known as Multan City. Multan City is home to a significant number of communities, business districts, and residential regions that contribute to the city's vitality. Since it is home to large government offices, educational facilities, hospitals, and commercial establishments, it is a hub of activity and services. Figure 4.10 shows that a region known as Jalalpur Pirwala, which is a popular destination for pilgrims who frequent the area, is also being developed on vegetation near the bottom of the map as we are progressing towards year 2050.

4.4.2 LST

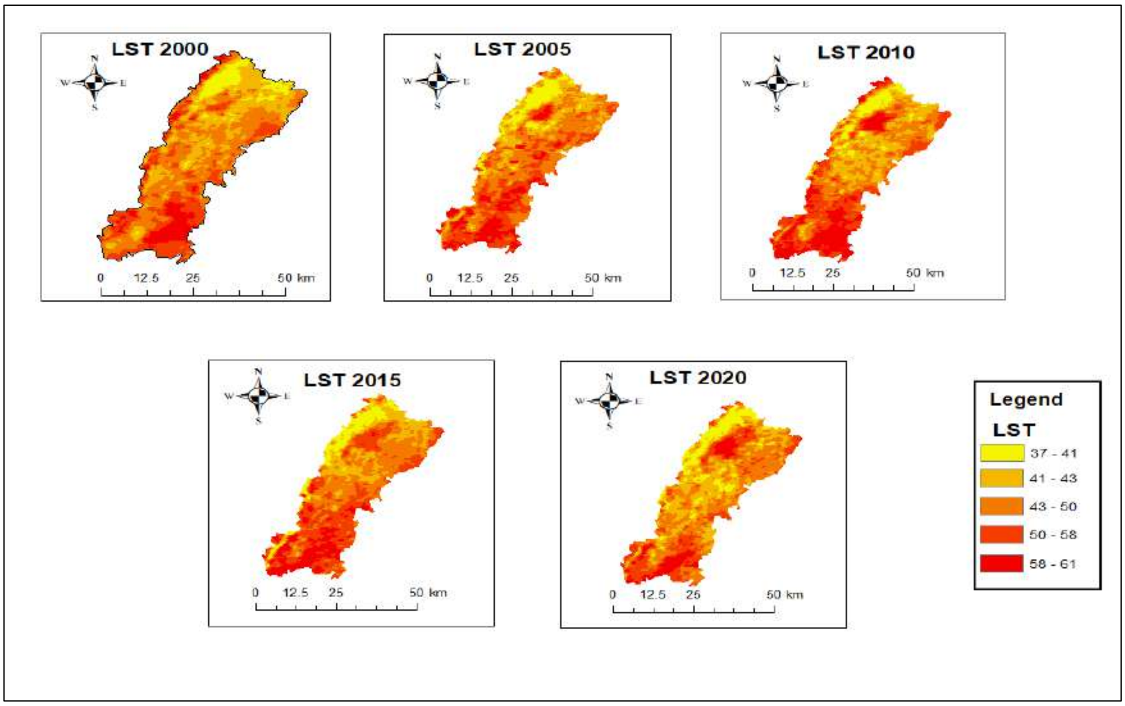

Figure4.11 LST of Multan from year 2000 to 2020.

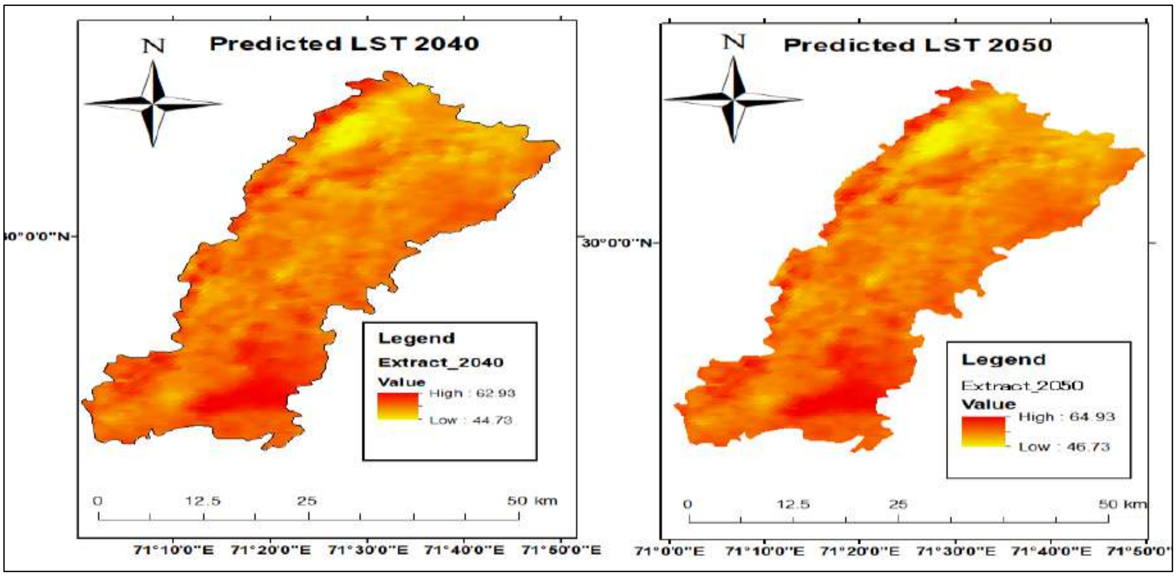

Figure4.12 Predicted LST of Multan for year 2040 and 2050.

Figure 4.11 makes it obvious that various Multan district locations, including Multan City and Jalalpur Pirwala, which are found at the top and bottom of the map, have high LST. Figure 4.12 illustrates that these areas have higher LST values than the other Multan District regions because they are more urbanized than the other region of the Multan District.

4.5 Faisalabad

<u>4.5.1 LULC</u>

Table4.4 LULC data for district Faisalabad.

Years	Temperature(℃)	Builtup(%)	vegetation(%)	Water(%)	Bareland(%)
2000	55.65	9.9	86.3	2.4	1.4
2005	57.35	10.4	85.9	2.2	1.5
2010	58.11	10.9	85.7	1.9	1.5
2015	58.39	11.9	85.2	1.1	1.8
2020	60.78	12.3	84.9	1.1	1.7
2040	62.12	51.4	46.4	0.7	1.5
2050	64.11	58.7	39.4	0.5	1.3

From table 4.4, there is a positive correlation between the passage of time and the increase in land surface temperature. As the built-up area has expanded from 9.9% to 58.7%, the land surface temperature has increased from 55.65℃ to 64.11℃. Simultaneously, there has been a decrease in vegetation area from 86.3% to 39.4%, water body from 2.4% to 0.5%, and bareland from 1.4% to 1.3%. These changes in land cover percentages indicate a trend of urbanization and the subsequent impact on temperature, resulting in an overall temperature increase over the past years.

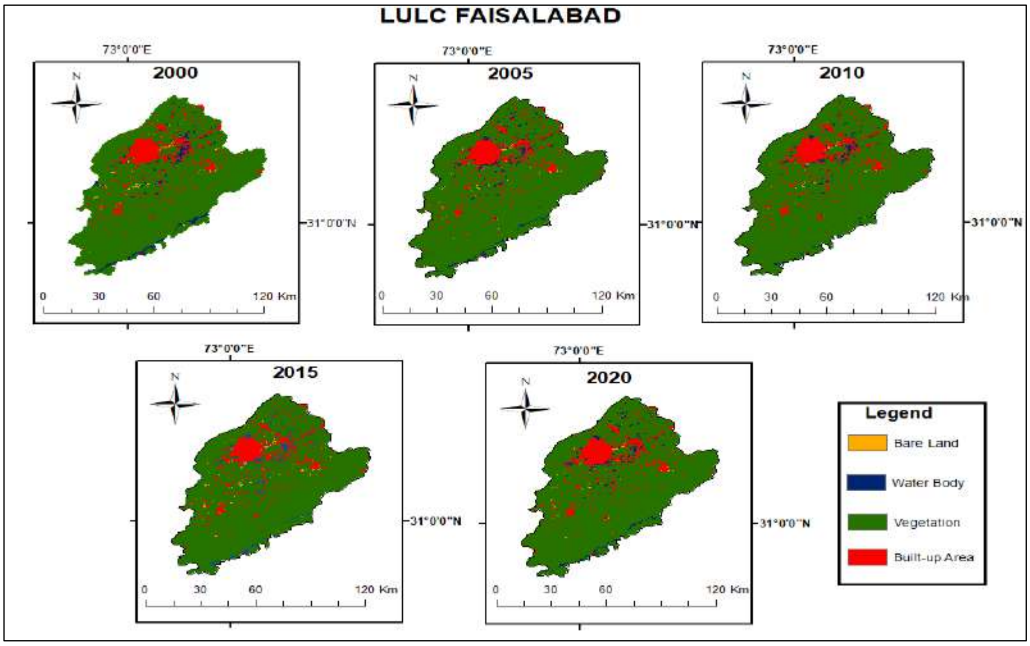

Figure4.13 LULC of Faisalabad for year 2000 to 2020.

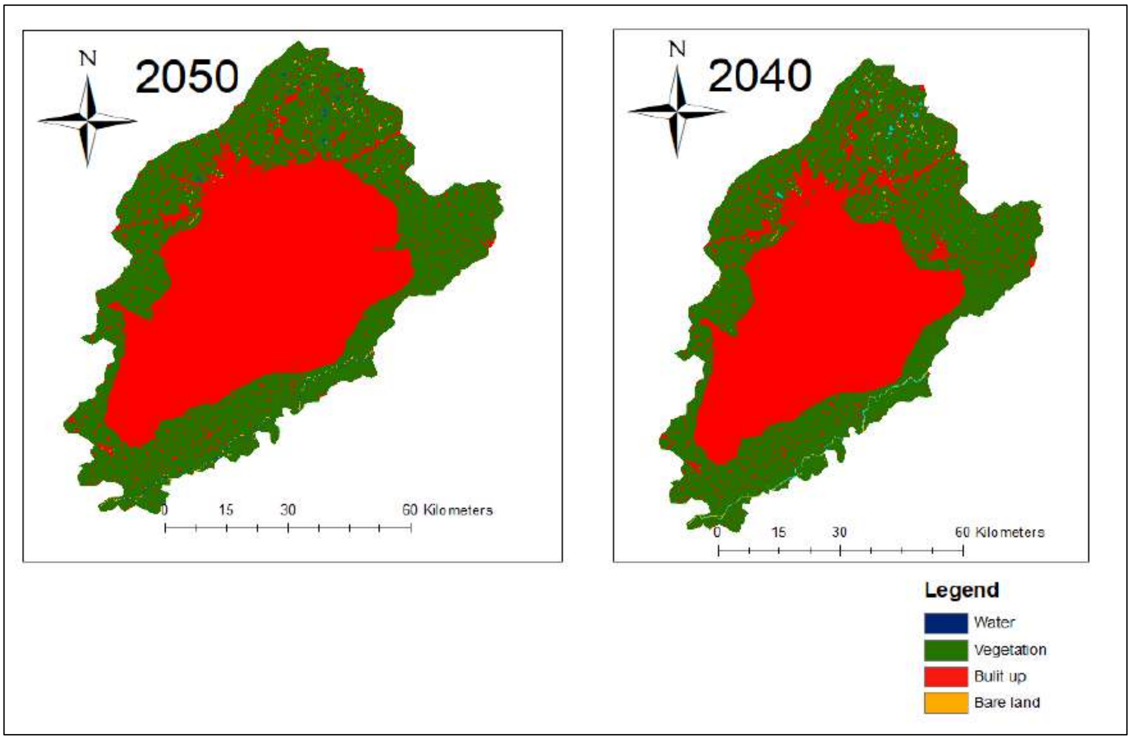

Figure4.14 Predicted LULC of Faisalabad for year 2040 and 2050.

As you can see in figure 4.13, the built-up region, or Saddar area, the centre of the Faisalabad district, is expanding on the top of the map. There is a greater need for residential, commercial, and industrial space as a result of the district's fast urbanization and population growth. Being the administrative and economic center of Faisalabad, the Saddar or city region has drawn a lot of investment and growth. It is a thriving and busy region because it is home to numerous businesses, markets, offices, and entertainment venues. The availability of significant road networks, transport facilities, and close proximity to industrial zones have all contributed to the growth of built-up regions in this area. As, we are progressing towards year 2050 it can be seen that the built area is increased rapidly around Saddar region as shown in figure 4.14 as well.

4.5.2 LST

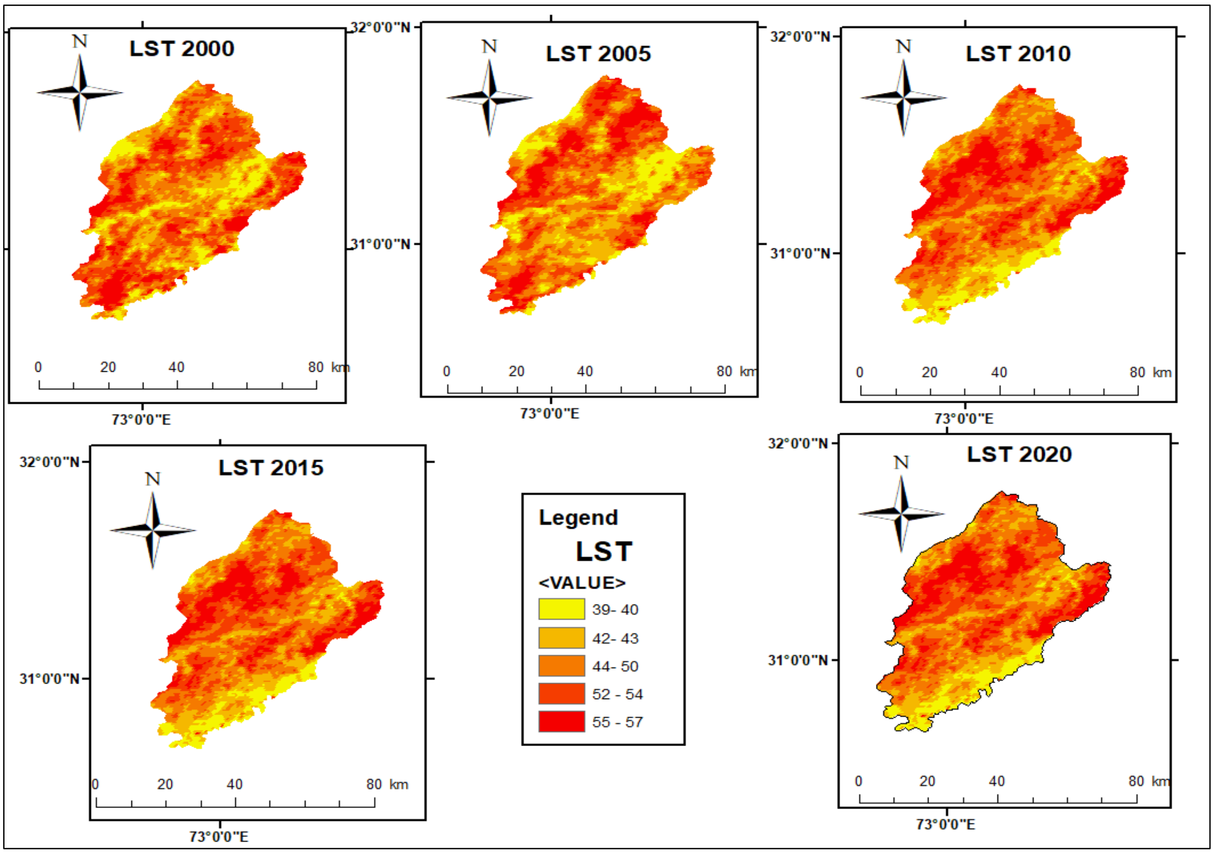

Figure4.15 LST of Faisalabad from year 2000 to 2020.

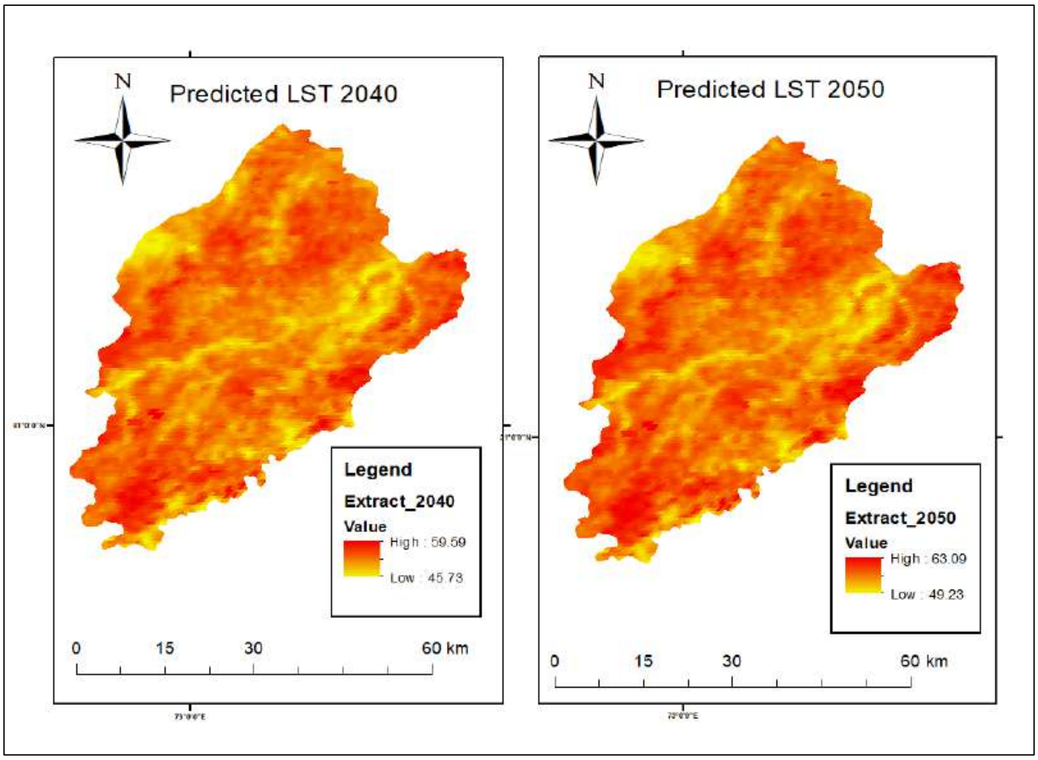

Figure4.16 Predicted LST of Faisalabad for year 2040 and 2050.

From figure 4.15, it can be seen clearly that the LST is increasing in and around Saddar region as we are progressing towards year 2020 because the availability of significant road networks, transport facilities, and close proximity to industrial zones have all contributed to the growth of built-up regions in this area as a result LST is higher as compare to its surrounding regions in future decades as well as shown in figure 4.16 as well.

Chapter 5

5.1 Conclusions

The purpose of this research was to develop an understanding of the patterns of urbanization and the consequences that are connected with them in the districts of Lahore, Rawalpindi, Faisalabad, and Multan from the years 2000 to 2020. We analyzed changes in land use and land cover (LULC) by using data from the USGS Landsat satellite. Additionally, we investigated the effects of urbanization on surface temperature, specifically the phenomenon known as the Urban Heat Island (UHI). Our research demonstrates that urbanization has a considerable negative effect on both the natural world and human health.

The study of LULC changes showed that there has been a discernible rise in surface temperature over the past two decades, with Rawalpindi witnessing a rise in temperature of 2 degrees Celsius, Multan and Lahore experiencing even higher rises at 2.4 degrees Celsius and 2.6 degrees Celsius respectively. This rise in temperature can be linked to the growth of built-up areas and the decrease in water bodies that has occurred in the study districts as a result of this growth. The findings highlight the negative impacts of urbanization, including greater rates of energy consumption and air pollution, in addition to the potential health hazards associated with higher temperatures.

In addition, we made our projections for the future surface temperature using an Artificial Neural Network (ANN), which covered the period from 2020 to 2050. According to the projections, each of the four districts will experience a significant rise in surface temperature. Temperature increases of 4 ºC, 2 ºC, 1.5 ºC, and 3.5 ºC are forecast for the cities of Lahore, Multan, and Rawalpindi, respectively, over the next few days. These estimates underline the critical need for effective urban planning methods to reduce the impacts of UHI and regulate the rapid pace of urbanization. These measures are urgently needed because urbanization is occurring at an alarming rate.

In order to solve these difficulties, politicians and urban planners should place an emphasis on environmentally responsible methods of urbanization. Shade, cooling, and an improvement in air quality are all benefits that can be reaped from the establishment and maintenance of green areas like parks, gardens, and urban forests, which can help reduce the impact of the urban heat island. Protecting and restoring water bodies can also play an important role in lowering surface temperatures and enhancing the overall urban environment. This is especially true if these efforts are coordinated.

The findings of this study highlight the significance of taking preventative actions to manage urbanization and limit the negative effects of urbanization. Policymakers and urban planners are able to make informed judgments in order to design plans for sustainable urbanization if they have a solid understanding of the changes to LULC and the expected temperature rises. The application of these solutions will make a contribution to the building of cities that are livable, resilient, and environmentally friendly, thereby improving the well-being of citizens and safeguarding the natural resources that are essential for a sustainable future.

5.2 Recommendations

Our recommendation regarding the project is as follow:

1. For future studies, it is suggested to include more parameters of urbanizations in the model to elaborate differences in LST for more reliable assessment.
2. Application of more machine learning techniques should be implemented.
3. To mitigate the urban heat island effect, potential solutions include decentralization, conservation of natural resources, eco-friendly, sustainable urban development plans, and promoting urban plantation may be evaluated.

References

[1] N. Ahmed *et al.*, “Climate change adaption strategies in urban communities: new evidence from Islamabad, Pakistan,” *Environ. Sci. Pollut. Res.*, pp. 1–14, 2023.

[2] A. Dilawar *et al.*, “Spatiotemporal shifts in thermal climate in responses to urban cover changes: a-case analysis of major cities in Punjab, Pakistan,” *Geomatics, Nat. Hazards Risk*, vol. 12, no. 1, pp. 763–793, 2021, doi: 10.1080/19475705.2021.1890235.

[3] G. Ulpiani, “On the linkage between urban heat island and urban pollution island: Three-decade literature review towards a conceptual framework,” *Sci. Total Environ.*, vol. 751, p. 141727, 2021, doi: 10.1016/j.scitotenv.2020.141727.

[4] Y. Y. Loo, L. Billa, and A. Singh, “Effect of climate change on seasonal monsoon in Asia and its impact on the variability of monsoon rainfall in Southeast Asia,” *Geosci. Front.*, vol. 6, no. 6, pp. 817–823, 2015, doi: 10.1016/j.gsf.2014.02.009.

[5] C. Fang, H. Liu, and G. Li, “International progress and evaluation on interactive coupling effects between urbanization and the eco-environment,” *J. Geogr. Sci.*, vol. 26, pp. 1081–1116, 2016.

[6] P. Fan, Z. Ouyang, D. D. Nguyen, T. T. H. Nguyen, H. Park, and J. Chen, “Urbanization, economic development, environmental and social changes in transitional economies: Vietnam after Doimoi,” *Landsc. Urban Plan.*, vol. 187, pp. 145–155, 2019.

[7] L. Liang, Z. Wang, and J. Li, “The effect of urbanization on environmental pollution in rapidly developing urban agglomerations,” *J. Clean. Prod.*, vol. 237, p. 117649, 2019.

[8] X. Yang, L. Zhao, M. Bruse, and Q. Meng, “An integrated simulation method for building energy performance assessment in urban environments,” *Energy Build.*, vol. 54, pp. 243–251, 2012, doi: 10.1016/j.enbuild.2012.07.042.

[9] A. Hsu, G. Sheriff, T. Chakraborty, and D. Manya, “Disproportionate exposure to urban heat island intensity across major US cities,” *Nat. Commun.*, vol. 12, no. 1, pp.

1–11, 2021, doi: 10.1038/s41467-021-22799-5.

[10] Shahfahad, S. Talukdar, M. Rihan, H. T. Hang, S. Bhaskaran, and A. Rahman, "Modelling urban heat island (UHI) and thermal field variation and their relationship with land use indices over Delhi and Mumbai metro cities," *Environ. Dev. Sustain.*, vol. 24, no. 3, pp. 3762–3790, 2022, doi: 10.1007/s10668-021-01587-7.

[11] V. K. Singh, J. A. Acero, and A. Martilli, "Evaluation of the impact of anthropogenic heat emissions generated from road transportation and power plants on the UHI intensity of Singapore," *Tech. Rep. Cool. Singapore*, vol. 500, 2020.

[12] S. Vujovic, B. Haddad, H. Karaky, N. Sebaibi, and M. Boutouil, "Urban heat island: Causes, consequences, and mitigation measures with emphasis on reflective and permeable pavements," *CivilEng*, vol. 2, no. 2, pp. 459–484, 2021.

[13] Jabbar and M. M. Yusoff, "Assessing the Spatiotemporal Urban Green Cover Changes and Their Impact on Land Surface Temperature and Urban Heat Island in Lahore (Pakistan) Research Paper," *Geogr. Environ. Sustain.*, vol. 15, no. 1, pp. 122–140, 2022, doi: 10.24057/2071-9388-2021-005.

[14] X. Li, Y. Zhou, S. Yu, G. Jia, H. Li, and W. Li, "Urban heat island impacts on building energy consumption: A review of approaches and findings," *Energy*, vol. 174, pp. 407–419, 2019, doi: 10.1016/j.energy.2019.02.183.

[15] A. Piracha and M. T. Chaudhary, "Urban air pollution, urban heat island and human health: a review of the literature," *Sustainability*, vol. 14, no. 15, p. 9234, 2022.

[16] S. Shabahang, B. Vale, and M. Gjerde, "A Simulation Method for Studying Urban Heat Islands at the Urban Scale," *Smart Innov. Syst. Technol.*, vol. 203, no. January, pp. 115–126, 2021, doi: 10.1007/978-981-15-8783-2_9.

[17] T. A. N. T. Perera, T. M. D. Nayanajith, G. Y. Jayasinghe, and H. D. S. Premasiri, "Identification of thermal hotspots through heat index determination and urban heat island mitigation using ENVImet numerical micro climate model," *Model. Earth Syst. Environ.*, vol. 8, no. 1, pp. 209–226, 2022, doi: 10.1007/s40808-021-01091-x.

[18] Z. Wang, "China Green Economy for Eco-urbanization in Urban-Rural Coordinated Development".

[19] S. Hosseinihaghighi, F. Izadi, R. Padsala, and U. Eicker, "Using climate-sensitive 3d city modeling to analyze outdoor thermal comfort in urban areas," *ISPRS Int. J. Geo-*

Information, vol. 9, no. 11, 2020, doi: 10.3390/ijgi9110688.

[20] M. T. Sohail, Y. Mahfooz, K. Azam, Y. Yen, L. Genfu, and S. Fahad, "Impacts of urbanization and land cover dynamics on underground water in Islamabad, Pakistan," *Desalin Water Treat*, vol. 159, pp. 402–411, 2019.

[21] M. Ahmad *et al.*, "Modelling the dynamic linkages between eco-innovation, urbanization, economic growth and ecological footprints for G7 countries: Does financial globalization matter?," *Sustain. Cities Soc.*, vol. 70, p. 102881, 2021, doi: https://doi.org/10.1016/j.scs.2021.102881.

[22] K. Ullah, S. Abbas, M. Tariq, N. Mahmood, and H. Kaechele, "The symmetric and asymmetric impacts of green energy, eco-innovation, and urbanization in explaining low-carbon economy for Pakistan," *Environ. Sci. Pollut. Res.*, vol. 30, no. 12, pp. 33375–33395, 2023.

[23] I. S. Elsayed, "Mitigation of the urban heat island of the city of Kuala Lumpur, Malaysia," *Middle-East J. Sci. Res.*, vol. 11, no. 11, pp. 1602–1613, 2012.

[24] J. Amanollahi, C. Tzanis, M. F. Ramli, and A. M. Abdullah, "Urban heat evolution in a tropical area utilizing Landsat imagery," *Atmos. Res.*, vol. 167, pp. 175–182, 2016.

[25] S. Kimothi *et al.*, "Spatio-temporal fluctuations analysis of land surface temperature (LST) using Remote Sensing data (LANDSAT TM5/8) and multifractal technique to characterize the urban heat Islands (UHIs)," *Sustain. Energy Technol. Assessments*, vol. 55, p. 102956, 2023.

[26] D. Armson, P. Stringer, and A. R. Ennos, "The effect of tree shade and grass on surface and globe temperatures in an urban area," *Urban For. Urban Green.*, vol. 11, no. 3, pp. 245–255, 2012, doi: https://doi.org/10.1016/j.ufug.2012.05.002.

[27] G. Levermore, J. Parkinson, K. Lee, P. Laycock, and S. Lindley, "The increasing trend of the urban heat island intensity," *Urban Clim.*, vol. 24, pp. 360–368, 2018.

[28] K. Deilami, M. Kamruzzaman, and Y. Liu, "Urban heat island effect: A systematic review of spatio-temporal factors, data, methods, and mitigation measures," *Int. J. Appl. Earth Obs. Geoinf.*, vol. 67, pp. 30–42, 2018, doi: https://doi.org/10.1016/j.jag.2017.12.009.

[29] A.- Al Kafy, M. S. Rahman, A.-A.- Faisal, M. M. Hasan, and M. Islam, "Modelling future land use land cover changes and their impacts on land surface temperatures in

Rajshahi, Bangladesh," *Remote Sens. Appl. Soc. Environ.*, vol. 18, p. 100314, 2020, doi: https://doi.org/10.1016/j.rsase.2020.100314.

[30] D. X. Tran, F. Pla, P. Latorre-Carmona, S. W. Myint, M. Caetano, and H. V Kieu, "Characterizing the relationship between land use land cover change and land surface temperature," *ISPRS J. Photogramm. Remote Sens.*, vol. 124, pp. 119–132, 2017, doi: https://doi.org/10.1016/j.isprsjprs.2017.01.001.

[31] M. S. Saleem, S. R. Ahmad, Shafiq-Ur-Rehman, and M. A. Javed, "Impact assessment of urban development patterns on land surface temperature by using remote sensing techniques: a case study of Lahore, Faisalabad and Multan district," *Environ. Sci. Pollut. Res.*, vol. 27, no. 32, pp. 39865–39878, 2020, doi: 10.1007/s11356-020-10050-5.

[32] P. Fu and Q. Weng, "A time series analysis of urbanization induced land use and land cover change and its impact on land surface temperature with Landsat imagery," *Remote Sens. Environ.*, vol. 175, pp. 205–214, 2016.

[33] S. Temperature *et al.*, "Remote Sensing-Based Prediction of Temporal Changes in Land," 2022.

[34] S. Hussain *et al.*, "Using GIS tools to detect the land use/land cover changes during forty years in Lodhran District of Pakistan," *Environ. Sci. Pollut. Res.*, vol. 27, pp. 39676–39692, 2020.

[35] S. Hussain *et al.*, "Assessment of land use / land cover changes and its effect on land surface temperature using remote sensing techniques in Southern Punjab , Pakistan," *Environ. Sci. Pollut. Res.*, no. 0123456789, 2022, doi: 10.1007/s11356-022-21650-8.

[36] M. Imran and A. Mehmood, "Analysis and mapping of present and future drivers of local urban climate using remote sensing: a case of Lahore, Pakistan," *Arab. J. Geosci.*, vol. 13, pp. 1–14, 2020.

[37] A. Tariq, F. Mumtaz, M. Majeed, and X. Zeng, "Spatio-temporal assessment of land use land cover based on trajectories and cellular automata Markov modelling and its impact on land surface temperature of Lahore district Pakistan," *Environ. Monit. Assess.*, vol. 195, no. 1, 2023, doi: 10.1007/s10661-022-10738-w.

[38] Z. Liu, W. Cheng, C. Y. Jim, T. E. Morakinyo, Y. Shi, and E. Ng, "Heat mitigation benefits of urban green and blue infrastructures: A systematic review of modeling

techniques, validation and scenario simulation in ENVI-met V4," *Build. Environ.*, vol. 200, p. 107939, 2021, doi: https://doi.org/10.1016/j.buildenv.2021.107939.

[39] M. H. Saputra and H. S. Lee, "Prediction of land use and land cover changes for north sumatra, indonesia, using an artificial-neural-network-based cellular automaton," *Sustainability*, vol. 11, no. 11, p. 3024, 2019.

[40] A. Dilawar *et al.*, "Spatiotemporal shifts in thermal climate in responses to urban cover changes: a-case analysis of major cities in Punjab, Pakistan," *Geomatics, Nat. Hazards Risk*, vol. 12, no. 1, pp. 763–793, 2021.

[41] S. Ullah, A. A. Tahir, T. A. Akbar, and Q. K. Hassan, "Remote Sensing-Based Quantification of the Relationships between Land Use Land Cover Changes and Surface Temperature over the Lower Himalayan Region".

[42] S. Khan, S. Gul, and W. Li, "Remote sensing evaluation of land surface temperature and urban area expansion in Zhengzhou city during 2013-2015," *Nat. Appl. Sci. Int. J.*, vol. 2, no. 1, pp. 39–55, 2021.

[43] S. Guha, H. Govil, A. Dey, and N. Gill, "Analytical study of land surface temperature with NDVI and NDBI using Landsat 8 OLI and TIRS data in Florence and Naples city, Italy," *Eur. J. Remote Sens.*, vol. 51, no. 1, pp. 667–678, 2018.

[44] M. Imran, A. Stein, and R. Zurita-Milla, "Using geographically weighted regression kriging for crop yield mapping in West Africa," *Int. J. Geogr. Inf. Sci.*, vol. 29, no. 2, pp. 234–257, 2015.

[45] G. Ali *et al.*, "Environmental impacts of shifts in energy, emissions, and urban heat island during the COVID-19 lockdown across Pakistan," *J. Clean. Prod.*, vol. 291, p. 125806, 2021, doi: 10.1016/j.jclepro.2021.125806.

[46] Q. Yang, Q. Yuan, L. Yue, T. Li, H. Shen, and L. Zhang, "The relationships between PM2. 5 and aerosol optical depth (AOD) in mainland China: About and behind the spatio-temporal variations," *Environ. Pollut.*, vol. 248, pp. 526–535, 2019.

[47] M. Imran and A. Mehmood, "Analysis and mapping of present and future drivers of local urban climate using remote sensing : a case of Lahore , Pakistan," 2020.

[48] M. S. Khan, S. Ullah, T. Sun, A. U. Rehman, and L. Chen, "Land-use/land-cover changes and its contribution to urban heat Island: A case study of Islamabad, Pakistan," *Sustain.*, vol. 12, no. 9, 2020, doi: 10.3390/su12093861.

[49] E. A. Alshari and B. W. Gawali, "Development of classification system for LULC using remote sensing and GIS," *Glob. transitions Proc.*, vol. 2, no. 1, pp. 8–17, 2021.

[50] T. Lillesand, R. W. Kiefer, and J. Chipman, *Remote sensing and image interpretation*. John Wiley & Sons, 2015.

[51] Z. Abbas and H. S. Jaber, "Accuracy assessment of supervised classification methods for extraction land use maps using remote sensing and GIS techniques," in *IOP Conference Series: Materials Science and Engineering*, 2020, vol. 745, no. 1, p. 12166.

[52] T. Jaman, K. Dharanirajan, and S. Rana, "Land use and Land cover Change detection and Its Environmental Impact on South Andaman Island, India using Kappa coefficient Statistical Analysis and Geospatial Techniques.".

[53] S. Mansour, M. Al-Belushi, and T. Al-Awadhi, "Monitoring land use and land cover changes in the mountainous cities of Oman using GIS and CA-Markov modelling techniques," *Land use policy*, vol. 91, p. 104414, 2020.

[54] Z. Abbas, G. Yang, Y. Zhong, and Y. Zhao, "Spatiotemporal change analysis and future scenario of LULC using the CA-ANN approach: a case study of the Greater Bay Area, China," *Land*, vol. 10, no. 6, p. 584, 2021.

[55] M. F. Baig, M. R. U. Mustafa, I. Baig, H. B. Takaijudin, and M. T. Zeshan, "Assessment of land use land cover changes and future predictions using CA-ANN simulation for selangor, Malaysia," *Water*, vol. 14, no. 3, p. 402, 2022.

[56] S. K. Dhull and K. K. Singh, "ECG beat classifiers: a journey from ANN to DNN," *Procedia Comput. Sci.*, vol. 167, pp. 747–759, 2020.

[57] R. N. Faragallah and R. A. Ragheb, "Evaluation of thermal comfort and urban heat island through cool paving materials using ENVI-Met," *Ain Shams Eng. J.*, vol. 13, no. 3, p. 101609, 2022.

[58] M. Kumari, K. Sarma, and R. Sharma, "Predicting Spatial and Decadal LULC Changes in the Singrauli District of Madhya Pradesh Through Artificial Neural Network Models Using Geospatial Technology," *J. Indian Soc. Remote Sens.*, pp. 1–12, 2022.